Science of the Total Environment

Toward Ecological Forecasting of West Nile Virus in Florida: Insights from Two Decades of Surveillance

--Manuscript Draft--

Manuscript Number:	
Article Type:	Research Paper
Keywords:	Vector-borne disease; Arbovirus, sentinel chickens; spatiotemporal modeling; Gaussian Markov random fields; stochastic partial differential equations
Corresponding Author:	Joseph Alex Baecher, Ph.D. University of Florida Vero Beach, Florida UNITED STATES
First Author:	Joseph Alex Baecher, Ph.D.
Order of Authors:	Joseph Alex Baecher, Ph.D.
	Vinod Anand Akshay, M.S.
	Guralnick Penn Robert, Ph.D.
	Amy M Bauer, Ph.D.
	Yasmin Nicolao Tavares, M.S.
	Yesenia Sánchez, B.S.
	James T Thorson, Ph.D.
	Lindsay P Campbell, Ph.D.
Abstract:	West Nile Virus (WNV) is the leading cause of mosquito-borne disease in the United States, yet transmission activity remains difficult to predict. This study used 20 years of digitized WNV seroconversion data from 526 sentinel chicken coops across Florida to develop spatiotemporal models with landscape and climate variables to predict WNV seroconversion at monthly and seasonal timescales. We found several environmental predictors hypothesized to impact WNV transmission were important at both timescales. Lower WNV seroconversion was predicted with higher maximum temperature during the sampling month and greater proportions of developed land cover, while intermediate values of minimum temperature at two-months prior predicted higher WNV seroconversion. In the seasonal model, intermediate values of cumulative precipitation one season prior predicted higher WNV seroconversion. High accuracy in out-of-sample predictions at both timescales demonstrates the utility of our models toward ecological forecasting of enzootic transmission. Monthly models had higher precision than the seasonal model, but both timescales have potential to inform management decisions. Monthly predictions could guide targeted control efforts during active transmission seasons, while seasonal predictions provide a lead-time to improve preparedness and inform resource allocation. Retrospective statewide predictions across the 20 year time period provided qualitative correlations between areas of high predicted WNV transmission hazard among humans and equines, while also providing insights into WNV transmission ecology following its introduction in 2001. Overall, our framework provides a step forward in the use of spatiotemporal ecological modeling for public health and vector-borne disease ecology and management.

Title:

Toward Ecological Forecasting of West Nile Virus in Florida: Insights from Two Decades of Surveillance

Authors:
J. Alex Baecher[1,3*], V. A. Akshay[2,3], Robert P. Guralnick[2,3,], Amy M. Bauer[4], Yasmin N. Tavares[1,4], Yesenia Sánchez[1], James T. Thorson[5], Lindsay P. Campbell[1,2,4*]

Affiliations:
[1]Florida Medical Entomology Laboratory, IFAS, University of Florida, Vero Beach, Florida 32962
[2]School of Natural Resources and Environment, IFAS, University of Florida, Gainesville, Florida 32611
[3]Florida Natural History Museum, University of Florida, Gainesville, Florida 32611
[4]Department of Entomology and Nematology, IFAS, University of Florida, Gainesville, Florida 32611
[5]Resource Ecology and Fisheries Management, Alaska Fisheries Science Center, Seattle, WA, 98115

ORCID:
J. Alex Baecher: 0000-0003-0247-5758
V. A. Ashay: 0000-0003-3554-7818
Robert P. Guralnick: 0000-0001-6682-1504
Amy M. Bauer: 0000-0002-6749-811X
Yasmin N. Tavares: 0000-0002-5369-1728
Yesenia Sánchez: 0009-0003-7682-7362
James T. Thorson: 0000-0001-7415-1010
Lindsay P. Campbell: 0000-0001-6069-1198

Corresponding author (*) correspondence:
Lindsay Campbell: lcampbell2@ufl.edu and J. Alex Baecher: jbaecher@gmail.com.

Author contributions:
LPC and **RPG:** Conceptualization, Funding acquisition, Supervision, Writing – Review & Editing; **VAA**, **AMB**, **YNS**, and **YT:** Data Curation, Writing – Review & Editing; **JAB:** Data curation, Formal analysis, Writing – Original Draft; **JT:** Software, Writing – Review & Editing.

Abstract: West Nile Virus (WNV) is the leading cause of mosquito-borne disease in the United States, yet transmission activity remains difficult to predict. This study used 20 years of digitized WNV seroconversion data from 526 sentinel chicken coops across Florida to develop spatiotemporal models with landscape and climate variables to predict WNV seroconversion at monthly and seasonal timescales. We found several environmental predictors hypothesized to impact WNV transmission were important at both timescales. Lower WNV seroconversion was predicted with higher maximum temperature during the sampling month and greater proportions of developed land cover, while intermediate values of minimum temperature at two-months prior predicted higher WNV seroconversion. In the seasonal model, intermediate values of cumulative precipitation one season prior predicted higher WNV seroconversion. High accuracy in out-of-sample predictions at both timescales demonstrates the utility of our models toward ecological forecasting of enzootic transmission. Monthly models had higher precision than the seasonal model, but both timescales have potential to inform management decisions. Monthly predictions could guide targeted control efforts during active transmission seasons, while seasonal predictions provide a lead-time to improve preparedness and inform resource allocation. Retrospective statewide predictions across the 20 year time period provided qualitative correlations between areas of high predicted WNV transmission hazard among humans and equines, while also providing insights into WNV transmission ecology following its introduction in 2001. Overall, our framework provides a step forward in the use of spatiotemporal ecological modeling for public health and vector-borne disease ecology and management.

Keywords: Vector-borne disease, Arbovirus, sentinel chickens, spatiotemporal modeling, Gaussian Markov random fields, Stochastic Partial Differential Equations

Acronym definitions: AIC = Akaike Information Criteria, API = Application Programming Interface, ARIMA = autoregressive integrated moving average, CPDE = conditional percent deviance explained, FDOH = Florida Department of Health, FCCMC = Florida Coordinating Council on Mosquito Control, GLMM = generalized linear mixed-model, GRF = Gaussian random fields, GMRF = Gaussian Markov random fields, INLA = Integrated Nested Laplace Approximation, LULC = land use land cover, NB = negative binomial, NLCD = National Land Cover Database, RMSE = root mean square error, SPDE = stochastic partial differential equations, TMB = Template Model Builder, WNV = West Nile virus.

1. Introduction:

Vector-borne diseases cause widespread mortality and morbidity worldwide, with more than 700,000 deaths each year (WHO, 2025). These disease systems include dynamic interactions among pathogens, vectors, and hosts that are determined by intrinsic multitrophic population dynamics and external environmental conditions (Pavlovskiĭ, 1966; Mordecai et al., 2019). Despite ongoing efforts, predicting transmission activity as a means to assess risk remains a persistent challenge given the inherent complexity of these systems (Kiryluk et al., 2024; Molina-Guzmán et al., 2022; Wang et al., 2024; Lauer et al., 2020). As a result, performant short-term (e.g., seasonal or monthly) forecasting has largely remained elusive, in part due to a lack of flexible and operational models that can integrate the right environmental conditions with multispecies dynamics at relevant spatiotemporal scales to predict virus activity. Consequently, prevention and control efforts are frequently reactive rather than proactive, identifying problems only after transmission has already occurred (Chung et al., 2013; Dye-Braumuller et al., 2022). A key next step for vector-borne disease prevention is the development of a predictive framework that can capture complex system dynamics and operate on timescales relevant to management decisions (Barker, 2019; Keyel et al., 2021).

Zoonotic vector-borne disease systems, in particular, are difficult to predict because often, multiple arthropod vectors and hosts are responsible for maintenance and spillover transmission in the natural environment (Rees et al., 2021; Roberts et al., 2021). West Nile virus (hereafter, “WNV”; Family: *Flaviviridae*, Genus: *Flavivirus*) is a multi-host, multi-vector zoonotic arbovirus maintained primarily in an enzootic cycle between ornithophilic *Culex* mosquitoes and passerine and columbiform birds with occasional spillover transmission to humans and other animals (Campbell et al., 2002; Reisen, 2013). WNV has global epidemiological relevance and is the leading cause of mosquito-borne disease in the USA, with a 10% mortality rate among neuroinvasive cases (Ciota, 2017). Given the human and veterinary health importance of WNV (CDC, 2024), multiple states including Florida, routinely monitor for WNV. For example, Florida Department of Health (FDOH) has maintained a decades-long surveillance effort, monitoring weekly WNV seroconversion in sentinel chickens across a wide geographic region and large portions of the year (FDOH, 2025; Fig. 1). This long-term monitoring program is unique because it is a targeted measure of virus activity in the natural environment, over a relatively large geographic area (state of Florida; Fig. 1), and has consistent collections over a 20 year time period (Lauer et al., 2020).

Since its arrival to North America in 1999, multiple studies have used shorter or longer time series data of mosquito abundance, WNV positive mosquito pools, human case data, and/or sentinel chicken seroconversion to understand, predict, or forecast WNV disease system dynamics with the environment at different spatiotemporal resolutions (Wimberly et al., 2014; Barker, 2019; Poh et al., 2019; Keyel et al., 2021; Wimberly et al., 2022; Ward et al., 2023), but few generalities have emerged (DeGroote et al., 2014). One challenge is that regional variation in mosquito vectors and hosts and the broad range of habitats and environments they occupy make predictions of the WNV system particularly complex (Kain & Bolker, 2019; Kilpatrick et al., 2006; Rochlin et al., 2019). A second challenge is that disease systems are not driven by environmental conditions alone (Mordecai et al., 2019), and individual field studies or short term monitoring efforts often fail to capture underlying spatiotemporal dynamics of hosts and vectors. The end result is that models often cannot accurately predict elevated WNV transmission hazard to inform management decisions (Holcomb et al., 2023).

Despite challenges, WNV dynamics are not fully stochastic (Campbell et al., 2022; Holcomb et al., 2023), and it may be possible to leverage spatiotemporal structure in unmeasured variables to improve model predictions (Reich et al., 2021; Hebert et al., 2024). Recent advances in provisioning of long term time series data and spatiotemporal (a.k.a., geostatistical) models provide the basis needed to model environmental conditions and spatiotemporal structure together to predict WNV system dynamics. While spatiotemporal modeling approaches are not new (Kyriakidis & Journel, 1999; Gelfand & Banerjee, 2017), a next generation of tools have been very recently developed that simultaneously simplify model specification and make accurate predictions (Wikle et al., 2019; Thorson & Kristensen, 2024). In particular, R packages such as *sdmTMB* (Anderson et al., 2024) and *tinyVAST* (Thorson et al., 2025) are capable of accounting for spatiotemporal interactions among variables and can fit non-linear dynamics, while still using model specifications that are well known to environmental scientists. Thus far, spatiotemporal modeling approaches have demonstrated utility in some WNV modeling efforts (Myer et al., 2017; Myer & Johnston, 2019; Campbell et al., 2022; McCarter et al., 2023; also see the “Global Burden of Disease Study” for the use of TMB models, e.g., Schumacher et al., 2024). Still these modeling tools, which are ideal for the WNV system given their complexity, remain underutilized in predicting transmission hazard across unsampled areas and at temporal resolutions useful for management decisions.

Previous investigations in Florida have used a combination of inference based and predictive approaches to examine environmental conditions and WNV, but similar to other regions of the U.S., often have varying results. Ecological niche models (ENMs) have been created to predict environmental suitability for WNV mosquito vectors, *Culex nigripalpus* and *Culex quinquefasciatus*, in St. Johns County in northeastern Florida (Sallam et al., 2016). Later, Beeman et al. (2021) used ENMs to predict environmental suitability of sentinel chicken seroconversion across Florida using aggregated coop data from 2014 – 2018. This model output was then used to further delineate habitats that may have greater WNV transmission hazard (Beeman et al., 2022). Tavares et al. (2024) found regional variation in the importance of landscape composition and configuration on WNV sentinel chicken seroconversion in 2018, including non-linear relationships between semi-urban landscapes and seropositive chickens in the central portion of Florida, but no consistent statewide predictors were identified. Higher proportions of WNV vector competent mosquitoes were predicted with greater percentages of developed landscapes across Manatee County, FL (Bauer et al., 2024), but Campbell et al. (2022) found landscapes were not strong predictors of 2018 sentinel chicken seroconversion in northeastern Florida. A time series study of human cases and sentinel chicken seroconversion suggested that drought periods followed by heavy precipitation precede WNV infections in both sentinel chickens and humans (Shaman et al., 2005). However, residual spatiotemporal autocorrelation was not assessed, and such correlations were found to be an important factor when modeling weekly 2018 sentinel chicken seroconversion in northeastern Florida (Campbell et al., 2022). There, best performing models included spatiotemporal terms, and initial strong support of lagged cumulative precipitation was no longer evident. In sum, relying on static models has been shown to be unlikely to yield either understanding of system dynamics or predictive accuracy. However, dynamic models are data hungry and require dense sampling in space and time to uncover environmental determinants or to make accurate predictions (Magurran et al., 2010; Solà et al., 2025).

The objective of this study is to develop a predictive modeling framework for WNV sentinel chicken seroconversion over a 20 year time period in Florida using spatiotemporal models, and also to infer environmental covariates associated with West Nile detection. Our approach is designed to explicitly leverage the strong spatial and temporal structure of the surveillance data with external environmental conditions to develop spatially targeted predictions of statewide transmission hazard. We develop predictive models over two relevant decision-making timescales (e.g., monthly and seasonally) and create statewide retrospective predictions from 2001 to 2019. Our goal is to assess the predictive performance of these models to inform proactive management decisions as a first step toward ecological forecasting of this important zoonotic arbovirus system.

2. Methods

2.1. Study area:

From north to south, Florida's climate ranges from subtropical to tropical, with warm temperatures all year and distinct wet (May – October) and dry (November – April) seasons. Since the start of the new millenium, a relevant timeframe for this study, the state has experienced overall warming, with rising minimum temperatures and shifting precipitation patterns (McNulty et al., 2023). Between 2006 and 2016, Florida saw a 19% increase in urban development and the conversion of natural and agricultural lands to developed uses (NOAA, 2016).

2.2. WNV surveillance data digitization:

The FDOH, in conjunction with mosquito control programs, has consistently monitored weekly WNV seroconversion and other mosquito-borne diseases in sentinel chicken flocks throughout large portions of the year (Fig. 1). Weekly blood samples were taken from chickens and viral RNA was detected via qPCR (FDOH, 2025). Reports of these assays along with other data and metadata were maintained in a combination of digital and physical, analog documents. The heterogeneity in format is due to different data management practices that have emerged due to technological advances.

Here, we focused on generating a consistently formatted set of time series data over many sites, covering a nearly twenty year time period, from 2001 to 2019. We developed a bioinformatics pipeline that helped automate collation, digitization, and quality control. Paper copies of reports were scanned and analyzed with Amazon Web Service *Textract* Optical Character Recognition (OCR) software to extract text and numerical data, which were organized in data tables by date, county, and sentinel chicken flock information (e.g. number of susceptible birds for the program each week). The resulting data were cleaned, formatted, and joined with WNV seroconversion results using *tidyverse* functions in R (Wickham et al., 2019) and *OpenRefine* software (Ham, 2013) to remove any errors or other artifacts from scanning and OCR. These data were then joined with georeferenced sentinel chicken coop sites provided by the FDOH. The final database contained information from 515,796 weekly reports of WNV seroconversion, across 526 monitoring sites (Fig. 1). These sites are located in 42 of Florida's 67 counties, providing a comprehensive assessment of the geographic distribution of WNV enzootic transmission within the state.

2.2.1. Preparing data for modeling:

WNV transmission occurs primarily between June and December in Florida, which we refer to as the "active season". Due to the consistency of transmission during the active season, the majority of sentinel chicken surveillance efforts take place during this period. Therefore, we limit our prediction of sentinel chicken seroconversion counts to this seasonal time period. We opted to produce WNV predictions at monthly and seasonal scales, which could provide near-term predictions at two timescales to inform management activities. We therefore aggregated weekly seroconversion data to each timescale by summing seropositive counts at each coop site and retaining the overall sampling effort across each timescale, and then each dataset was subsetted into a training data set for model fitting and a hold-out data set for testing out-of-sample predictions. For the monthly dataset, the hold-out data set included the final two years of the time series (2018 – 2019), which provided 14 sampling months. For the active season data set, the final four years of the time series (2015 – 2019) served as the hold-out data for out-of-sample prediction.

2.3. Environmental data:

2.3.1. Climate:

Gridded (raster) 1-km^2 estimates of daily cumulative precipitation and minimum and maximum temperature were gathered for Florida from Daymet climate data (Thornton et al., 2022) between the years 2000 and 2020 (accessed via a Daymet API in R package *climateR*; Czernecki et al., 2025). Variables were then aggregated from daily to the monthly or seasonal temporal resolution by calculating average maximum and minimum temperature and the sum of cumulative precipitation (R package *terra;* Hijmans, 2025). Point estimates were extracted by location and date for each monitoring site during the study duration (R package *sf*; Pebesma & Bivand, 2023). Because seroconversion rates may be influenced by prior conditions (e.g, precipitation events or temperature from weeks or months before a positive sample), temporal lags were calculated for each climatic variable. For both the seasonal and monthly datasets, one- and two-timestep lags were calculated, resulting in seasonal weather lags of six months and one year, and monthly lags of one and two months.

2.3.2. Land use land cover:

Land use land cover (LULC) data were extracted at 30 m^2 resolution for all available time periods from the National Land Cover Database (NLCD; 2001, 2004, 2006, 2008, 2011, 2016, and 2019; Dewitz, 2024) using the R package *fedData* (Bocinsky et al., 2025). LULC data were reclassified to "developed", "natural", and "wetland" land cover classes (see SI 2.1 for reclassification) and then assigned to seasonal and monthly WNV seroconversion datasets using NLCD data from years nearest to the date of sampling. Next, 2.5 km diameter circular buffers were created to calculate the proportion of "developed", "natural", and "wetland" land cover classes surrounding each chicken coop site over the study period. To generate the same landscape variables for model prediction across Florida, we calculated the pixel-wise proportion of each LULC class within a 2.5 km^2 circular moving window, using a nearest neighbor function, resulting in a statewide gridded percent land cover dataset at 1 km^2 resolution (R package *terra*).

2.4. Statistical analysis

2.4.1. Model development:

The spatiotemporal modeling framework used in this study belongs to a class of spatiotemporal generalized linear mixed effects models (GLMM; Diggle & Gabriel, 2010) that explicitly account for spatiotemporally autocorrelated data using latent Gaussian random fields (GRF; Rue & Held, 2005). However, the use of GRFs presents substantial computational challenges due to costly covariance functions. Stochastic partial differential equations (SPDE) can be used to minimize the scale of this problem by approximating GRFs as Gaussian Markov Random fields (GMRF) with a Matérn covariance function (Lindgren et al., 2011; Krainski et al., 2018). This solution has been adopted by the Integrated Nested Laplace Approximation software (*INLA*; Rue et al., 2009), and later implemented in Template Model Builder software (*TMB*; Thorson et al., 2015). Here we use *sdmTMB* (Anderson et al., 2024), an R software package which integrates both *INLA* and *TMB* functionality, to model and predict spatiotemporal patterns of WNV sentinel chicken seroconversion counts as a function of climate conditions and different LULC types.

A structured protocol was used to determine the optimum parameterization of monthly and seasonal models. Because of the large number of environmental and lagged environmental variables, we first fitted a set of univariate GLMMs to identify variables that were not informative to WNV seroconversion. These models were fitted with a negative binomial residual distribution (NB1), log link function, fixed effect covariate for sampling effort, and random effect structure featuring nested random intercepts for the county and site of each chicken coop (R package *glmmTMB*; Brooks et al., 2025). Predictors included in these univariate models were parameterized as both linear and 2nd order polynomial terms. Monthly or seasonal WNV seroconversion counts at each coop site served as the response variable and our landscape or climate variables served as univariate environmental predictors. Predictor variables with 95% confidence intervals that did not cross zero were retained for further analysis. Next, we created a full model including all retained environmental variables and implemented backward stepwise model selection in the R package *buildmer* (Voeten, 2023) to identify a best performing model based on likelihood ratio tests. Multicollinearity between environmental predictors in the best performing model was then assessed using variance inflation factor (VIF) values (R package *car*; Fox & Weisberg, 2018), and variables with VIF values > 5 were then iteratively removed to meet model assumptions of independence. Finally, model performance was examined using checks for model convergence, posterior predictive checks, residual normality, and overdispersion (R packages *DHARMa* and *performance*; Hartig, 2025 and Lüdecke et al., 2021, respectively). We also report conditional percent deviance explained (CPDE), number of fixed effects, and effective degrees of freedom of random effects (Zheng et al., 2024) in SI Table 1.

Next, we fitted a spatiotemporal model to address spatiotemporal autocorrelation and make predictions in space and time at unsampled locations. To fit a spatiotemporal model using the SPDE approach, piecewise linear basis functions are computed using a Delaney triangulation over the spatial area of interest, commonly referred to as a “mesh” (Krainski et al., 2018). To establish a “mesh” for this study area, first a spatial domain was created by generating a 1-km diameter buffer around Florida and estimating a nonconvex hull (R package *INLA*; Rue et al., 2025). Next, the following parameters were used to adjust the structure and vertex density of the mesh with R package *fmesher* (Lindgren, 2025): “cutoff” (minimum triangle size), “max edge” (maximum triangle edge length), and “offset” (size of inner and outer spatial extensions around individual coordinates). These parameters were tuned following conventional practices detailed in Bakka et al., 2018, which suggests adjusting parameters by a factor of the spatial extent of the study area.

The spatiotemporal model developed in this study shares a basic anatomy with non-spatial GLMMs, but as the name indicates, the model requires additional terms to account for spatiotemporal non-independence. Here, we apply a Gaussian Markov spatiotemporal random field structures $\boldsymbol{\zeta}$ and $\boldsymbol{\epsilon}$ to account for spatio-temporal and spatial autocorrelation, respectively. The full model specification is therefore:

$$for\ s\ in\ 1 : N_{locations}\ and\ t\ in\ 1 : N_{timepoints}\ ...$$

$$y_{s,t} \sim ExpDist(\mu_{y_{s,t}},\ \varphi),$$

$$\mathbb{E}\left[y_{s,t}\right] = f^{-1}(\mathbf{X}^{\top}_{s,t}\boldsymbol{\beta} + \boldsymbol{Z}^{\top}_{s,t}\boldsymbol{Q} + \alpha_g + \boldsymbol{\zeta}_{s,t} + \boldsymbol{\epsilon}_s),$$

$$\alpha_g \sim N(0,\ \sigma^2_{\alpha}),$$

$$\boldsymbol{\zeta}_{t=1} \sim MVN(\mathbf{0},\ \boldsymbol{\Sigma}_{\epsilon}),$$

$$\boldsymbol{\zeta}_{t>1} = \rho\,\boldsymbol{\zeta}_{t-1} + \sqrt{1-\rho^2}\,\boldsymbol{\epsilon}_{\mathbf{t}},$$

$$\boldsymbol{\epsilon}_{\mathbf{t}} \sim MVN(\mathbf{0},\ \boldsymbol{\Sigma}_{\epsilon}), \qquad \text{(Eq. 2)}$$

where $\mathbb{E}$ is the expected mean of the response data y at point s and time t; μ represents the mean of the inverse link function f^{-1}; $\mathbf{X}$ and $\boldsymbol{Z}$ are two-dimensional design matrices at point s and time t, which are transposed (T) to take the inner-product with these elements and a vector of fixed- and random-effect coefficients $\boldsymbol{\beta}$ and $\boldsymbol{Q}$, respectively; α represents a random-intercept structure by groups g; $\boldsymbol{\epsilon}_{s,t}$ represents spatiotemporal random field at time $\mathbf{t}$ and location s; ζ represents deviations (or knots) of $\boldsymbol{\epsilon}_{\mathbf{t}}$ with a first-order autoregressive $AR(1)$ structure; $\boldsymbol{\Sigma}_{\epsilon}$ represents the covariance matrix of the spatiotemporal random field $\boldsymbol{\epsilon}$; and ρ represents the correlation between consecutive stationary random fields $\boldsymbol{\epsilon}$ at time t.

2.4.2. Model training, evaluation, and prediction:

Two spatiotemporal models were fitted to the monthly and seasonal training data sets with the model structure and climatic and land cover covariates described above using *sdmTMB* (Anderson et al., 2024). Once fitted, the models were evaluated using the same diagnostics as the non-spatiotemporal models and by examining parameter values, including extreme eigenvalues, standard errors, or random field variances, using the sanity check functionality in *sdmTMB*. To determine if the fixed effect environmental predictors and spatiotemporal structures (GMRF) improved model performance, marginal Akaike Information Criterion (AIC) was used to compare our spatiotemporal models (containing both GMRF and fixed and random effects) against two alternative null models: (*i*) a spatial random effect model (with GMRF but no environmental predictors) and (*ii*) a non-spatial random effect model (with no GMRF or environmental predictors). To evaluate these predictive accuracy, we calculated root mean square error (RMSE) and log likelihoods of out-of-sample predictions of sentinel chicken seroconversion counts for the monthly and the seasonal models (see SI Table 2 for out-of-sample log-likelihoods).

Finally, to determine how well these models can predict overall WNV activity (i.e., total active season or monthly counts), we derived seasonally- and monthly- aggregated predictions of WNV seropositive counts to a single statewide value. However, obtaining spatially-aggregated model predictions requires calculating non-linear functions which can produce biases that accumulate during aggregation, resulting in reduced predictive accuracy (Thorson & Kristensen, 2016). To obtain accurate predictions of total WNV seroconversion counts, we applied the "epsilon bias-correction estimator" (Thorson & Kristensen, 2024) for obtaining time-specific predictions of total WNV seroconversion and associated uncertainty (see SI 2.2 for bias-correction details). Next, fitted models were used to predict monthly and active season WNV seroconversion counts across unsampled areas across the state between 2001 and 2019. Due to computational intensity, the epsilon correction method was not applied to statewide prediction counts (i.e., Fig. 3 – 5).

All analyses after data assembly were conducted in the R programming environment (v4.4; R Core Team, 2025). All sentinel chicken data processing was performed on a personal computer with 8 CPUs and 32 GB RAM (processor: AMD Ryzen 3 3200U, 2.6 GHz). When compiling gridded environmental variables, fitting models using SPDE, or applying the epsilon bias-correction estimator, analyses were performed on a computing cluster with 10 – 20 CPUs and 80 – 160 GB RAM (processor: 9600 AMD EPYC 75F3 Milan, 3.0 GHz) on the University of Florida's Research Computing system's "HiPerGator 3.0".

3. Results

We digitized and formatted FDOH WNV sentinel chicken seroconversion surveillance data over a 20 year time period and used these data, knowledge of WNV system ecology, and spatiotemporal models to predict WNV transmission hazard across the state. Results from univariate GLMMs retained 18 candidate predictors for the monthly model and 22 candidate predictors for the seasonal model, including both landscape and climate variables with linear and polynomial terms (see SI 2.1 for variable reduction details). Following backward stepwise selection and removal of multicollinear environmental predictors, the final monthly and seasonal models each included 4 predictor variables (see Table 1 for a description of predictor variables). Results from the spatiotemporal models including GMRF and environmental predictors performed overwhelmingly better than null models with GMRF alone ($\Delta AIC_{monthly} = 1014.94$ and $\Delta AIC_{seasonal} = 414.82$; increasing CPDE by 14% for monthly models and 3% for seasonal models), as well as non-spatiotemporal models with the same predictors ($\Delta AIC_{monthly} = 4314.66$ and $\Delta AIC_{seasonal} = 16681.28$; with a 6- and 20-fold increase in monthly and seasonal CPDE, respectively). These results demonstrate the value of including both climate and landscape conditions and underlying spatiotemporal structure when modeling WNV sentinel chicken seroconversion (for AIC and CPDE values, see SI Table 1).

The main goal of this study was to develop spatiotemporal models that could accurately predict sentinel chicken seroconversion at future time periods. Both monthly and seasonal models showed high accuracy in out-of-sample prediction tests, supporting their utility toward ecological forecasting and decision-making at two temporal scales. Fig. 2 shows plots of model fits and predicted values during out-of-sample testing years (monthly: 2018 – 2019; seasonal: 2016 – 2019). While uncertainty was greater in out-of-sample predictions, values matched the direction and general magnitude of the empirical data, suggesting both models are capable of generalizing beyond the calibration data. In particular, hold-out empirical data sets for both models fell within the 95% CI of out-of-sample prediction. While both models performed well, the monthly model had greater accuracy and lower uncertainty than the seasonal model (Table 1), with over two-fold lower $RMSE$ when predicting to out-of-sample WNV seroconversion counts ($RMSE_{monthly} = 0.69$; $RMSE_{seasonal} = 2.19$). Overall, both seasonal and monthly models predicted marginally higher counts than the empirical data across the entire study period, including across the out-of-sample test data.

Multiple environmental predictors in the monthly and seasonal models were important to WNV sentinel chicken seroconversion, including lagged climate predictors that can help to provide lead times for management decisions (Fig. 1). In the monthly model, WNV seroconversion decreased as the proportion of human developed land cover surrounding chicken coops increased and as maximum temperatures increased during the month of sampling. In addition, model results showed a non-linear and two-month lagged response of WNV seroconversion to minimum temperatures, with higher seroconversion counts predicted at intermediate minimum temperature values. The seasonal model showed a similar result, but with intermediate cumulative precipitation values at a one-season lag, or over the six month period prior to the sampling season, predicting higher seroconversion. These results provide near-term environmental predictors of seroconversion that can be leveraged at two time periods to inform elevated transmission hazard.

Statewide retrospective predictions from 2001 to 2019 provided insights into the timing and distribution of WNV activity during the critical time period following its introduction to naive host populations (2001 – 2004) and subsequent establishment as an endemic virus system in the state (2005 – 2019; Fig. 4). In subsequent years, additional periods of elevated seroconversion were predicted at mid-latitudes in 2005 and again from 2010 to 2015. Statewide predictions at the monthly scale provide finer temporal resolution of these predictions (Fig. 4), including intra-seasonal diffusion of WNV on the northeastern Atlantic Coast near the cities of St. Augustine, Palm Coast, and Daytona Beach in 2014 and the Gulf Coast at Tampa and St. Petersburg in 2015. Spatial patterns of monthly predictions differed from seasonal patterns, often highlighting predicted enzootic WNV activity in urban and coastal regions (Fig. 5), particularly in southeastern Florida (e.g., the Miami-Fort Lauderdale-West Palm Beach metropolitan areas). For monthly predictions throughout the study period (2001 – 2019), see SI Fig. 1. Retrospective predictions of mean sentinel chicken seroconversion and associated uncertainty across the study period show greater uncertainty in areas with fewer sampling sites (Figs. 1 and 4).

4. Discussion

Building performant predictive models for multi-host, multi-vector zoonotic arbovirus systems is a key challenge to the development of effective prevention and control programs (Barker, 2019; Holcomb et al., 2023; Harp et al., 2025). Here, we leveraged long-term and spatially extensive sentinel chicken surveillance data to develop predictive spatiotemporal models of WNV transmission hazard in Florida over a 20 year time period. We found that both monthly and seasonal timescales were relevant and accurate for prediction, demonstrating strong utility toward ecological forecasts of WNV transmission hazard. Overall, this framework can serve as a basis for developing new operational tools to enhance targeted mosquito control and public health efforts (Barker, 2019; Keyel et al., 2021), while also advancing knowledge about the transmission ecology of this system.

4.1. A framework for predicting enzootic transmission

A key strength of our study lies in the extensive, long-term WNV sentinel chicken surveillance data, which captures statewide virus activity in the natural environment over a 20 year time period. Furthermore, the fine spatial (point-based) and temporal (weekly reports) resolution of these data allowed us to incorporate local climate and landscape data across a relatively broad geographic area, as well as to aggregate temporal records for near-term predictions of transmission hazard. These results further highlight that disease system dynamics can operate at multiple spatiotemporal scales, and harnessing these structures at different scales can provide tools with alternative but complementary predictive ability to inform transmission hazard (Garabed et al., 2020). Here, monthly predictions provide short-term and fine-scale information that could guide targeted control efforts during the active season, while seasonal predictions allow a lead-time ahead of the active season to improve preparedness and inform resource allocation across the state.

Differences in the importance of environmental predictors between monthly and seasonal models further highlight the utility of this approach. Land use and temperature were important predictors of seroconversion in monthly models, while only precipitation was predictive at the seasonal scale. Specifically, higher maximum temperatures in the sampling month is associated with lower seroconversion, while intermediate minimum temperatures two months prior to sampling predicted higher seroconversion. This result at this temporal scale is not surprising, given the critical role of temperature and thermal optima across mosquito life stages, where conditions that are too cold or too hot can reduce performance and lead to mortality (Gilbert & Raworth, 1996). In addition, greater percentages of developed landscapes surrounding chicken coops predicted lower seroconversion counts, but only in monthly models. The role of human developed landscapes in the WNV system has been studied extensively (Crowder et al., 2013; DeGroote et al., 2014; Eisen et al., 2010; Ezenwa et al., 2007; Ruiz et al., 2007), often with inconsistent results (Bowden et al., 2011; DeGroote et al., 2014). Here, our findings partially align with Tavares et al. (2024), who found that intermediate levels of developed land cover were important to 2018 WNV sentinel chicken seroconversion, but only in central Florida. Our results align less well with Bauer et al. (2024), who found higher proportions of WNV competent vectors predicted across more developed landscapes. However, Bauer et al. (2024) did not include host feeding behavior, an important factor when considering transmission hazard in the natural environment (Dahlin et al., 2024; Wen et al., 2015). In Florida, the primary mosquito vectors (*Culex quinquefasciatus* and *Culex nigripalpus*) and avian hosts are commonly found across gradients of developed areas, in addition to other habitats (Rochlin et al., 2019; Bauer et al., 2024; Day et al., 2015; Johnson et al., 2012). Here, our spatiotemporal framework may be capturing fine-scale, unmeasured ecological dynamics of vectors and hosts across these habitats, such as host and mosquito resource tracking across developed environments at the monthly scale.

Our finding that intermediate values of cumulative precipitation at a one season lag predicted higher WNV seroconversion may reflect overall increased availability of aquatic habitats required for mosquito development prior to the active transmission season (Nosrat et al., 2021). Excessive precipitation is known to result in larval flushing (Koenraadt & Harrington, 2008; Gardner et al., 2012), while drought conditions can reduce available habitats (Brown et al., 2014), which may reduce overall mosquito abundances. This result contrasts with previous studies in Florida suggesting that high precipitation following drought conditions precede WNV sentinel chicken and human infections (Shaman et al. 2005). This result may reflect the ability of our spatiotemporal models to account for autocorrelation in error terms that can sometimes mirror seasonal patterns (Ives, 2022). Overall, our model results show that overall mosquito habitat availability earlier in the season is likely important to the WNV disease system in Florida, and temperature and landscape at more proximal timescales are more informative predictors of sentinel chicken seroconversion. This outcome demonstrates that leveraging environmental conditions across multiple spatiotemporal scales can help to provide a more complete and potentially more process-driven understanding of enzootic transmission dynamics.

4.2. Retrospective predictions

Retrospective predictions of WNV seroconversion can provide valuable baselines for understanding past transmission hazards, especially when models capture dynamics effectively. Although many factors contribute to human WNV risk and disease (Barker, 2019), model outputs suggest clear qualitative correlations between predictions of elevated transmission hazard and human and equine WNV cases (accessed via FDOH's "Florida Arbovirus Surveillance" at floridahealth.gov). For example, in 2014 a total of 18 human infections and five equine infections occurred along the northeastern Atlantic coast of Florida, which corresponds directly with our predictions of elevated transmission hazard in this region (Fig. 4). The following year, human and equine cases were detected on the Gulf Coast near St. Petersburg, which also corresponded to elevated transmission hazard predicted in our seasonal model (Fig. 4). In 2011, multiple WNV equine cases were concentrated along the southwestern Gulf Coast, aligning with predictions of elevated transmission hazard (Fig. 4). Previous studies linking sentinel chicken infections to epidemiological outcomes have shown variable utility, with some studies indicating that enzootic transmission can serve as a warning for human infections (Kwan et al., 2010, 2012; Amdouni et al., 2020; Streng et al., 2024), while other studies found report delays or discordance with human outbreaks (Cherry et al., 2001; Gleiser et al., 2007). More work is needed to understand how enzootic and epizootic transmission align spatially and temporally, but we argue that stronger modeling frameworks for both may help with understanding the strength of association between the two cycles. Because our active season models provide a six month lead time for predictions of enzootic activity, our model outputs may provide a useful tool that can be used to better understand links between predicted transmission hazard in the natural environment and epidemiological outcomes.

Retrospective predictions from 2001 to 2003 also provide unique insights into the transmission ecology of WNV following its introduction and spread across naive host populations in Florida (Fig. 4). Our predictions in Florida align with other observations of a three year cycle of introduction, emergence, and subsidence (Reisen, 2013), with elevated transmission hazard predicted across much of Florida in 2002. Multiple zoonotic arboviruses maintained between avian hosts and mosquito vectors have recently emerged or expanded in geographic range, including Usutu virus in Europe (Vilibic-Cavlek et al., 2020) and Japanese encephalitis virus in Australia (McGuinness et al., 2023), and WNV continues to move into new geographic areas in Europe (Koch et al., 2024; Brüssow & Figuerola, 2025). Here, our model outputs may be informative toward understanding the invasion ecology of WNV in other geographic locations with similar environments, or to provide insights into future pathogen introductions that may be on the horizon. Early detection combined with robust spatiotemporal modeling provides a valuable resource that can be used to improve public health preparedness under future pathogen invasions.

4.3. Limitations, conclusions, and future directions

Despite the strengths of this study, limitations and opportunities for future development remain. Model performance is inherently influenced by the spatial heterogeneity of the underlying data, with greater predictive confidence in regions where sentinel chicken surveillance was more comprehensive (Fig. 1 and 5). Thus, uncertainty in our predictions are greatest in regions that are either sparsely sampled or entirely unsampled. Given this observation, future work should evaluate the generalizability of these models to other regions and time periods, particularly those with differing ecological or climatic contexts, where current model assumptions may not hold. Model outputs can be used to optimize design changes in monitoring to better capture the broadest environmental and geographic contexts (Oyafuso et al., 2021). Expanding data collection and analyses to a broader national or global scale holds promise, but would require a substantial increase in efforts towards surveillance to ensure robust calibration and validation. However, it may be possible to integrate model outputs with regional models from other areas as a means to provide the tools needed to develop broader applications. Building infrastructure to support real-time assimilation of new seroconversion data, as well as to integrate near-term climate forecasts, would also greatly enhance the utility of this framework. Finally, we see value in adapting recent developments in diffusion-enhanced spatiotemporal modelling (Lindgren et al., 2023), and integrating non-local covariates (i.e., climatological teleconnections), as well as mosquito trap collections and host species abundances to further enhance model results. Ultimately, our modeling framework can serve as the foundation for an operational ecological forecasting system to support proactive vector-borne disease management. While challenges remain, our framework is a step forward in the use of spatiotemporal ecological modeling for public health and vector-borne disease ecology and management.

Conflicts-of-interests: University of Florida Research Opportunity Seed Fund

Acknowledgements: This study was funded by the University of Florida Research Opportunity Seed Fund. We thank Dr. Jonathan Day, Bradley Eastmond, Florida Department of Health, and all mosquito control district personnel for thousands of hours of maintenance, sample collection, and testing of sentinel chicken flocks, as well as providing access to these data.

Data availability statement: All code necessary to conduct these analyses are stored in the following Github repository: https://github.com/slamander/chickens. Georeferenced sentinel chicken seroconversion data is available upon request through the Florida Department of Health Arbovirus Surveillance program upon agreement from participating Florida mosquito control programs through a memorandum of understanding. The authors did not receive special privileges in accessing the data that other researchers would not have. Contact information for data requests are available through the FDOH website: https://www.floridahealth.gov/diseases-and-conditions/mosquito-borne-diseases/surveillance.html.

TABLES:

Table 1: Description of the predictor variables used to model spatiotemporal WNV seroconversion counts in the state of Florida (USA). Models are defined at two temporal scales, monthly and seasonally. Terms included in this table result from a model selection and variable reduction procedure. Descriptions and parameterization details are provided for each variable.

Model	Effect	Term	Description	Variable type	Parameterization
Monthly	Fixed	*prcp*	Cumulative precipitation	Continuous	2^{nd} order orthogonal polynomial
		tmin_lag2	Min temperature (2 mo. lag)	Continuous	2^{nd} order orthogonal polynomial
		tmax	Max temperature (current)	Continuous	2^{nd} order orthogonal polynomial
		developed	Proportion developed land	Continuous	2^{nd} order orthogonal polynomial
		testing	Average sampling effort	Continuous	Linear predictor
	Random	*county*	County name	42-level factor	Intercept nested above ID
		ID	Monitoring site name	526-level factor	Intercept nested below county
Seasonal	Fixed	*prcp*	Cumulative precipitation	Continuous	2^{nd} order orthogonal polynomial
		prcp_lag2	Cumulative precipitation (12 mo. lag)	Continuous	2^{nd} order orthogonal polynomial
		tmax_lag2	Max temp (2-step lag)	Continuous	2^{nd} order orthogonal polynomial
		tmin_lag2	Min temp (2-step lag)	Continuous	2^{nd} order orthogonal polynomial
		testing	Average sampling effort	Continuous	Linear predictor
	Random	*county*	County name	42-level factor	Intercept nested above ID
		ID	Monitoring site name	526-level factor	Intercept nested below county

Table 2. Summary of model predictive accuracy when predicting out-of-sample West Nile Virus seroconversion counts during the active season (June – December). Predictive accuracy is measured using root mean square error (RMSE) and reported at both the annual (overall active season) and interannual periods (active season months) between 2016 and 2019, as well as the overall study period (Total). RMSE values are distinguished between predictions made from models fitted to monthly- and seasonally-aggregated active season data. Monthly RMSE ranges are derived from the minimum and maximum monthly RMSE values.

Year	**Out-of-sample prediction accuracy (RMSE)**	
	Seasonal	**Monthly (range)**
2016	1.02	NA
2017	1.13	NA
2018	3.05	0.73 (0.18, 1.04)
2019	2.75	0.65 (0.16, 0.99)
Total	2.19	0.69

Table 3. Summary of parameter estimates of predictors from a generalized mixed-effect spatiotemporal model WNV seroconversion counts in the state of Florida (USA). Models are defined at two temporal scales, monthly and seasonally. Predictors with parameter confidence intervals ("Lower" and "Upper" bounds) that do not overlap with zero (i.e., homogenous effects) are labeled with an asterisk and are considered important predictors of WNV seroconversion dynamics.

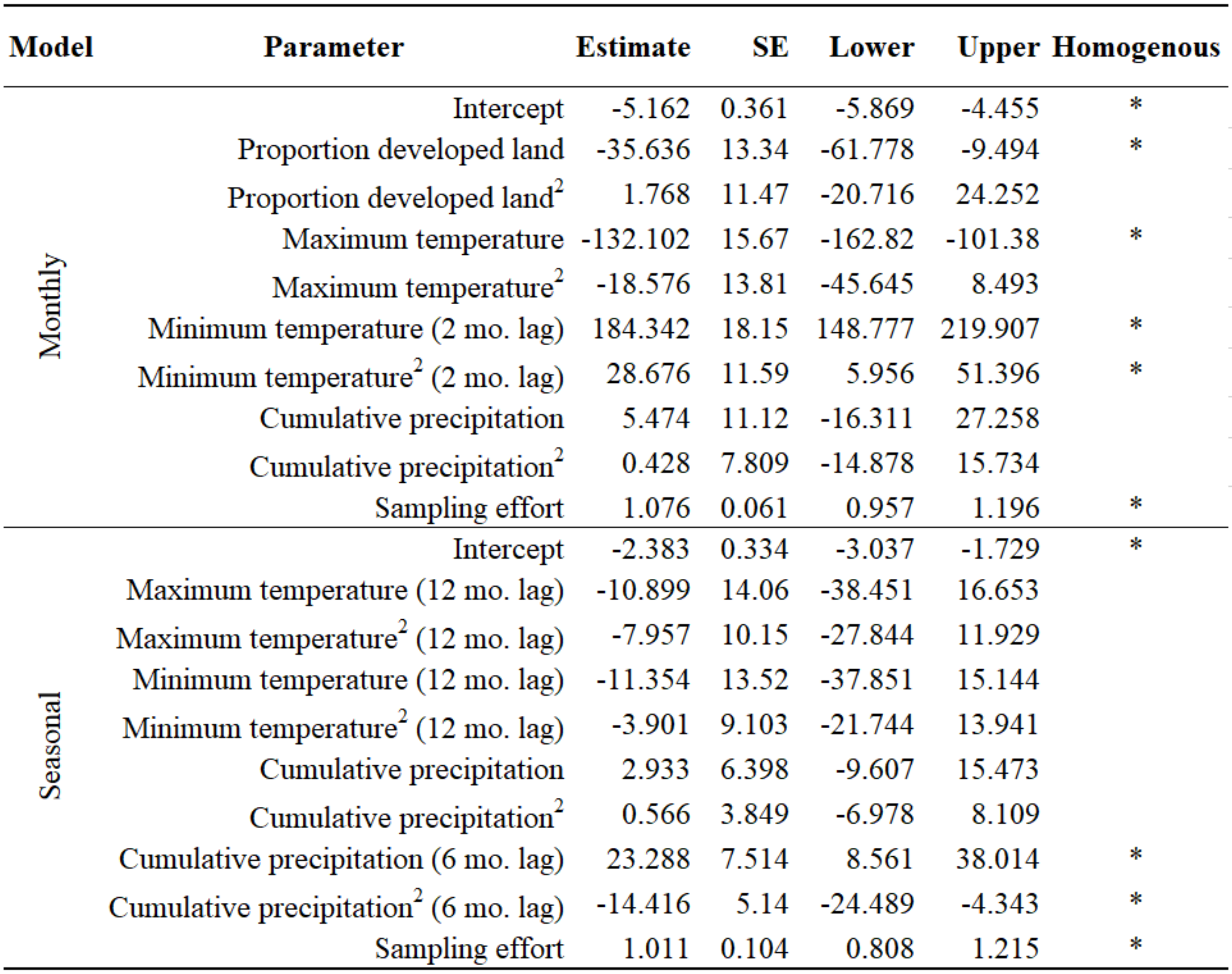

Model	Parameter	Estimate	SE	Lower	Upper	Homogenous
Monthly	Intercept	-5.162	0.361	-5.869	-4.455	*
	Proportion developed land	-35.636	13.34	-61.778	-9.494	*
	Proportion developed land^2	1.768	11.47	-20.716	24.252	
	Maximum temperature	-132.102	15.67	-162.82	-101.38	*
	Maximum temperature^2	-18.576	13.81	-45.645	8.493	
	Minimum temperature (2 mo. lag)	184.342	18.15	148.777	219.907	*
	Minimum temperature^2 (2 mo. lag)	28.676	11.59	5.956	51.396	*
	Cumulative precipitation	5.474	11.12	-16.311	27.258	
	Cumulative precipitation^2	0.428	7.809	-14.878	15.734	
	Sampling effort	1.076	0.061	0.957	1.196	*
Seasonal	Intercept	-2.383	0.334	-3.037	-1.729	*
	Maximum temperature (12 mo. lag)	-10.899	14.06	-38.451	16.653	
	Maximum temperature^2 (12 mo. lag)	-7.957	10.15	-27.844	11.929	
	Minimum temperature (12 mo. lag)	-11.354	13.52	-37.851	15.144	
	Minimum temperature^2 (12 mo. lag)	-3.901	9.103	-21.744	13.941	
	Cumulative precipitation	2.933	6.398	-9.607	15.473	
	Cumulative precipitation^2	0.566	3.849	-6.978	8.109	
	Cumulative precipitation (6 mo. lag)	23.288	7.514	8.561	38.014	*
	Cumulative precipitation^2 (6 mo. lag)	-14.416	5.14	-24.489	-4.343	*
	Sampling effort	1.011	0.104	0.808	1.215	*

FIGURES:

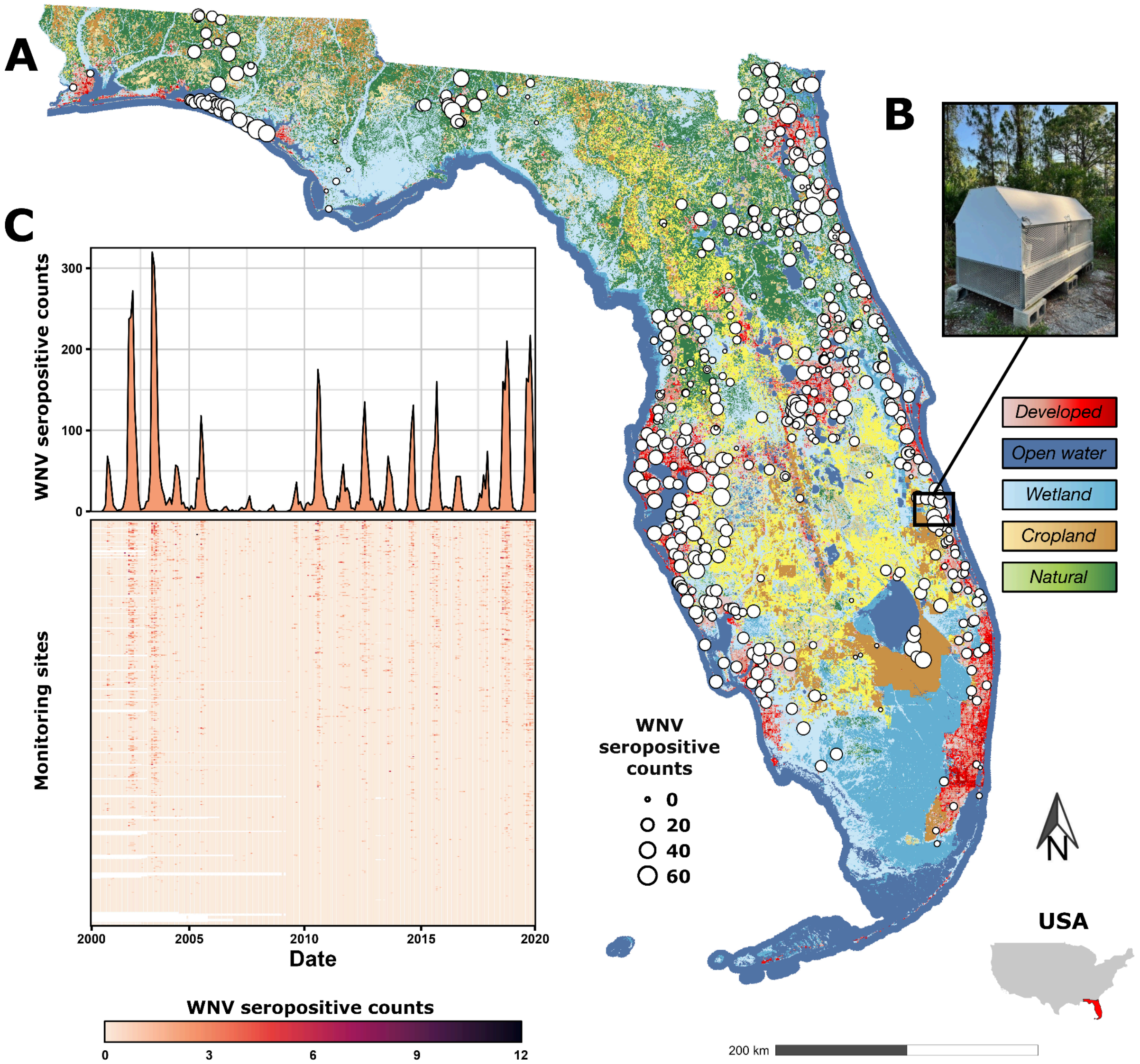

Fig. 1. Depiction of the data provided by the WNV seroconversion surveillance program operated by the state of Florida's Department of Health and many many mosquito control districts. (A) The spatial distribution and quantity of WNV seroconversion counts overlayed on a land cover land use map of Florida, detailing the proportion cover of urban development (red), open water (pelagic, dark blue), wetlands (light blue), cropland (yellow), and natural cover (green); (B) an example of the sentinel chickens coops from which the weekly seroconversion reports are generated; (C) a temporal summary of the seroconversion data, including (top) a line plot of monthly aggregated sums and (bottom) a Hovmöller diagram of the seroconversion data by locations of sentinel chickens coops ($N = 526$). Inset image (B) source: Indian River Mosquito Control District (https://www.irmosquito.com/sentinel-program).

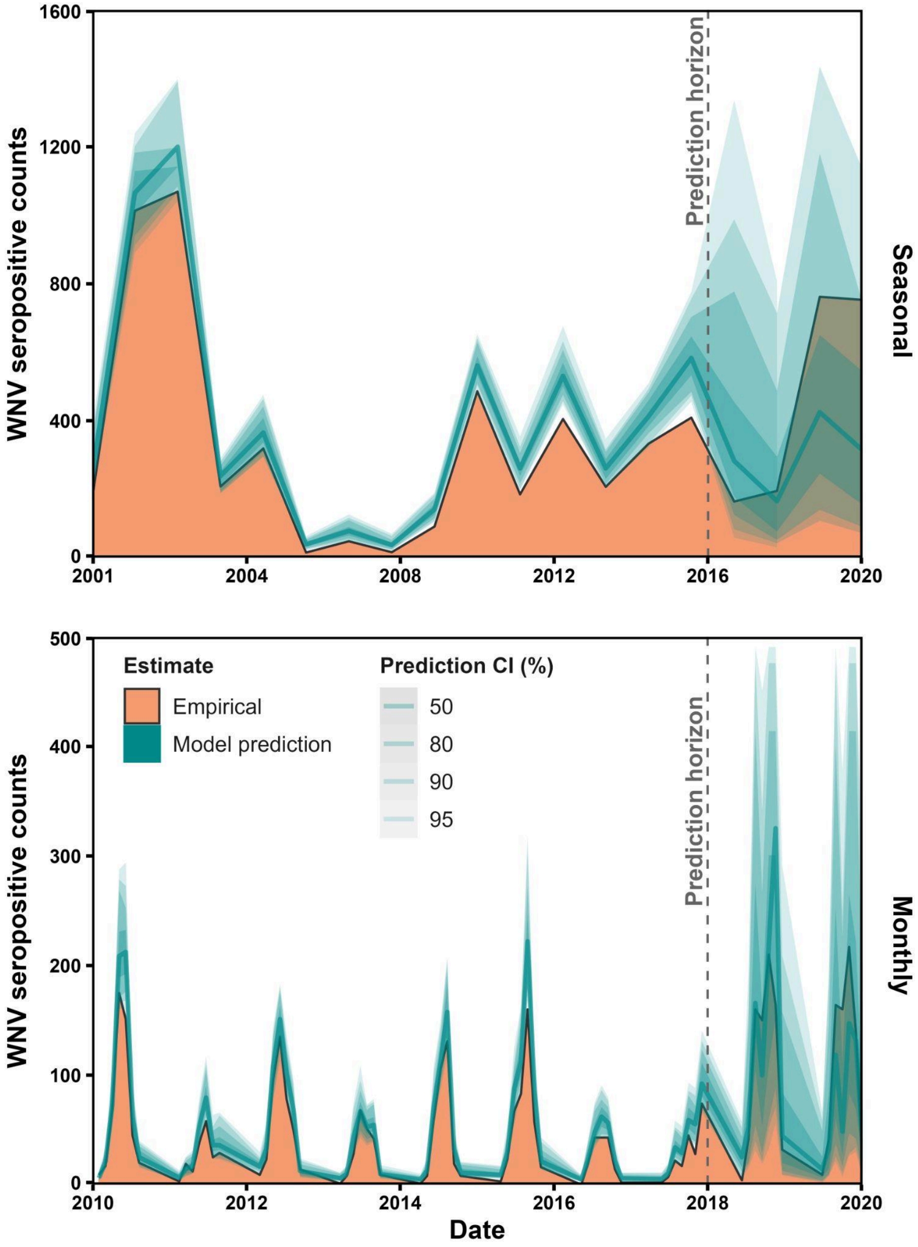

Fig. 2. Temporal trends of WNV seropositive counts in Florida (USA) from 2001 to 2019 estimated from empirical data (orange) and model-derived predictions (cyan). Empirical data were temporally aggregated by summing to the monthly (bottom panel) and seasonal (top panel) levels. The predictive performance of spatiotemporal models fitted to these two aggregated datasets were determined by predicting on hold-out data, which included the final two years of monthly data and the final four years of seasonal data (see dotted line indicating the beginning of the out-of-sample prediction horizon). Model predictions are presented as point-estimates (dark cyan line) and 50, 80, 90, and 95% confidence intervals (opaque cyan ribbons). The monthly panel's timeline is limited to 2010 – 2020 for ease of visualization, although models were fitted to the full time period of 2001 – 2019.

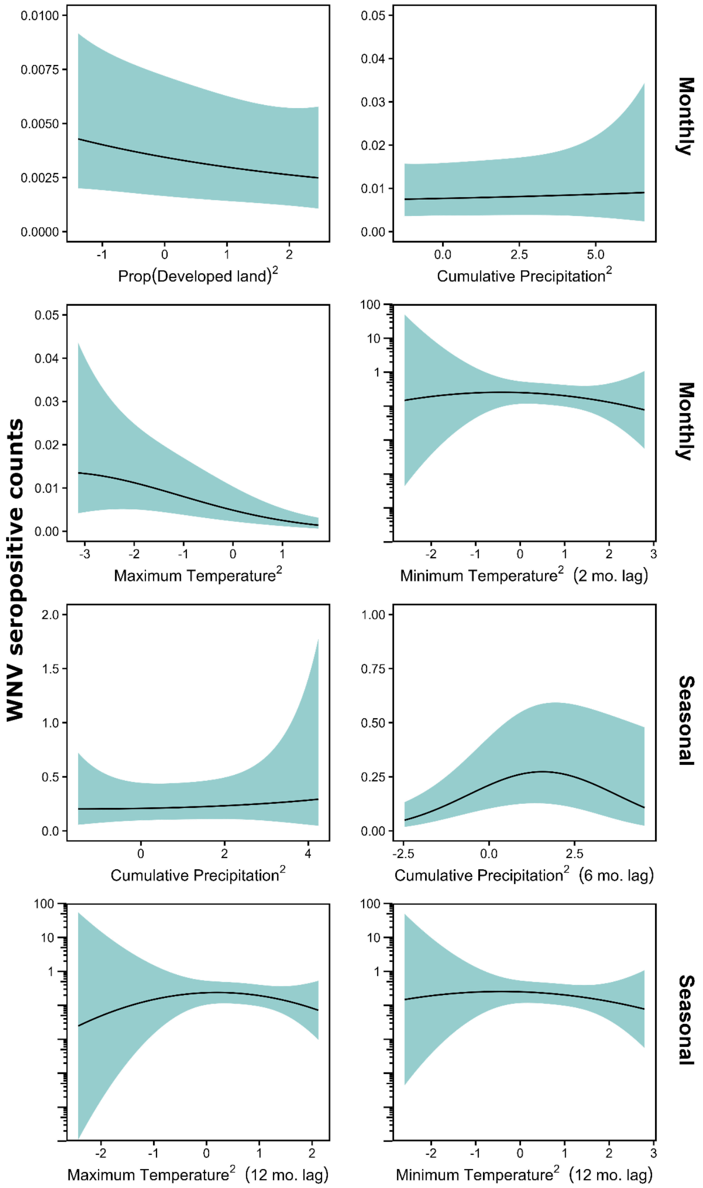

Fig. 3. Marginal response plots of predicted West Nile virus (WNV) seroconversion counts to environmental covariates. Predictions were obtained from a spatiotemporal model fitted to data from a sentinel chicken system in Florida from 2001 to 2019. Predictions were made from models fitted either to data aggregated to either the seasonal-level, including the months of the WNV active season (June – December), or to the monthly-level of the same activity period. Environmental covariates were either calculated from time periods that were contemporaneous with the response variable or temporally lagged by 1 to 2 time periods, indicated by the monthly lag in the variable name which is 1 – 2 months for monthly data and 6 – 12 months for seasonal data. Response plots are displayed in the “response” space, except for three panels displayed in the “link” space for ease of visualizing patterns.

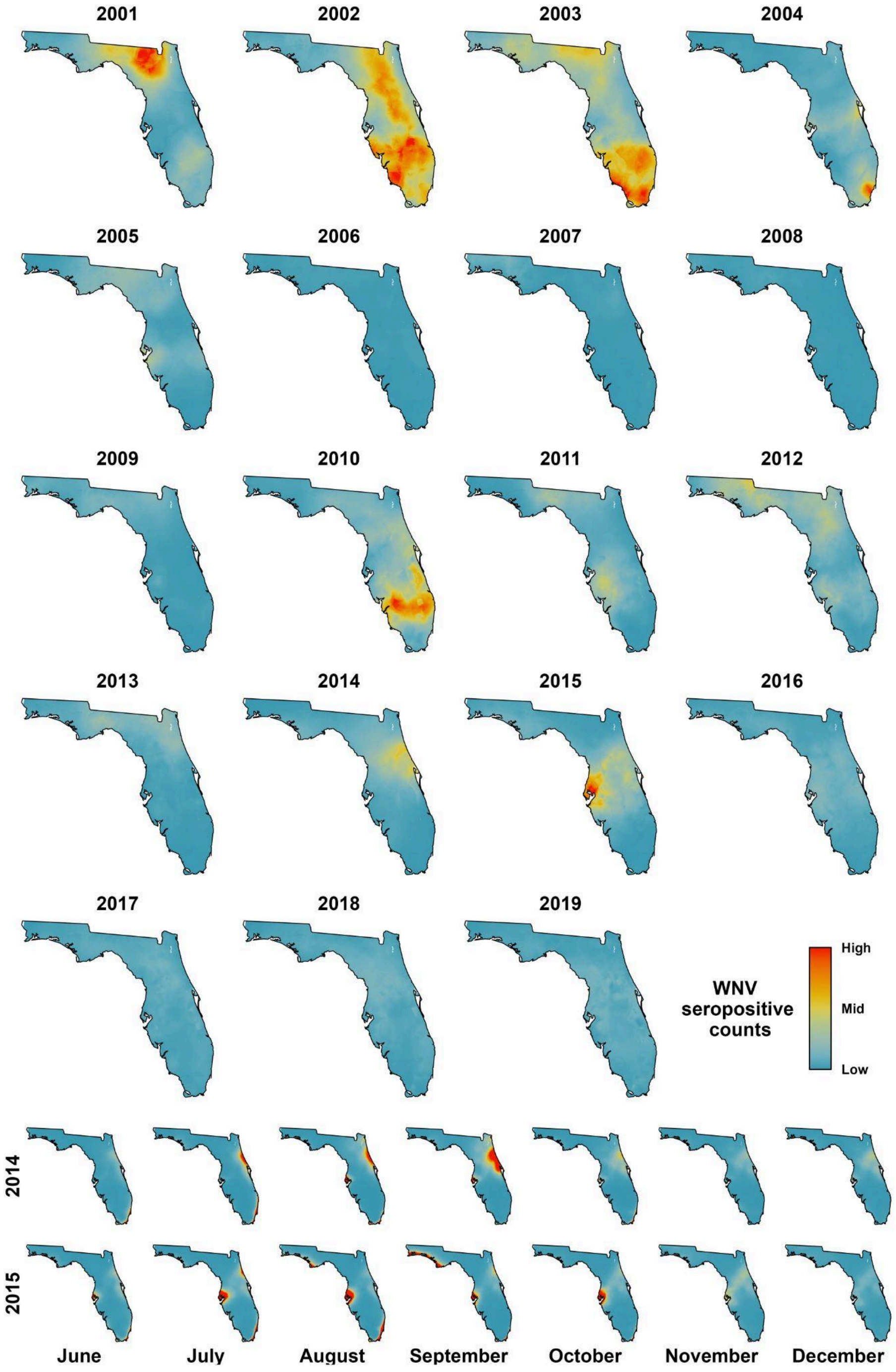

Fig. 4. Statewide predictions of the spatiotemporal dynamics of West Nile Virus seropositive counts from the Florida sentinel chicken system during the years of 2001 – 2019. Predictions were obtained from spatiotemporal models fitted to data aggregated to both seasonal (top panel) and monthly (bottom) temporal scales of the WNV activity season (June – December). An example of monthly predictions are provided for active months during the years of 2014 and 2015 (14 of the total 133 temporal periods). All predictions are provided with a quantile truncation for ease of visualization (seasonal: 99.9th percentile; monthly: 98th percentile).

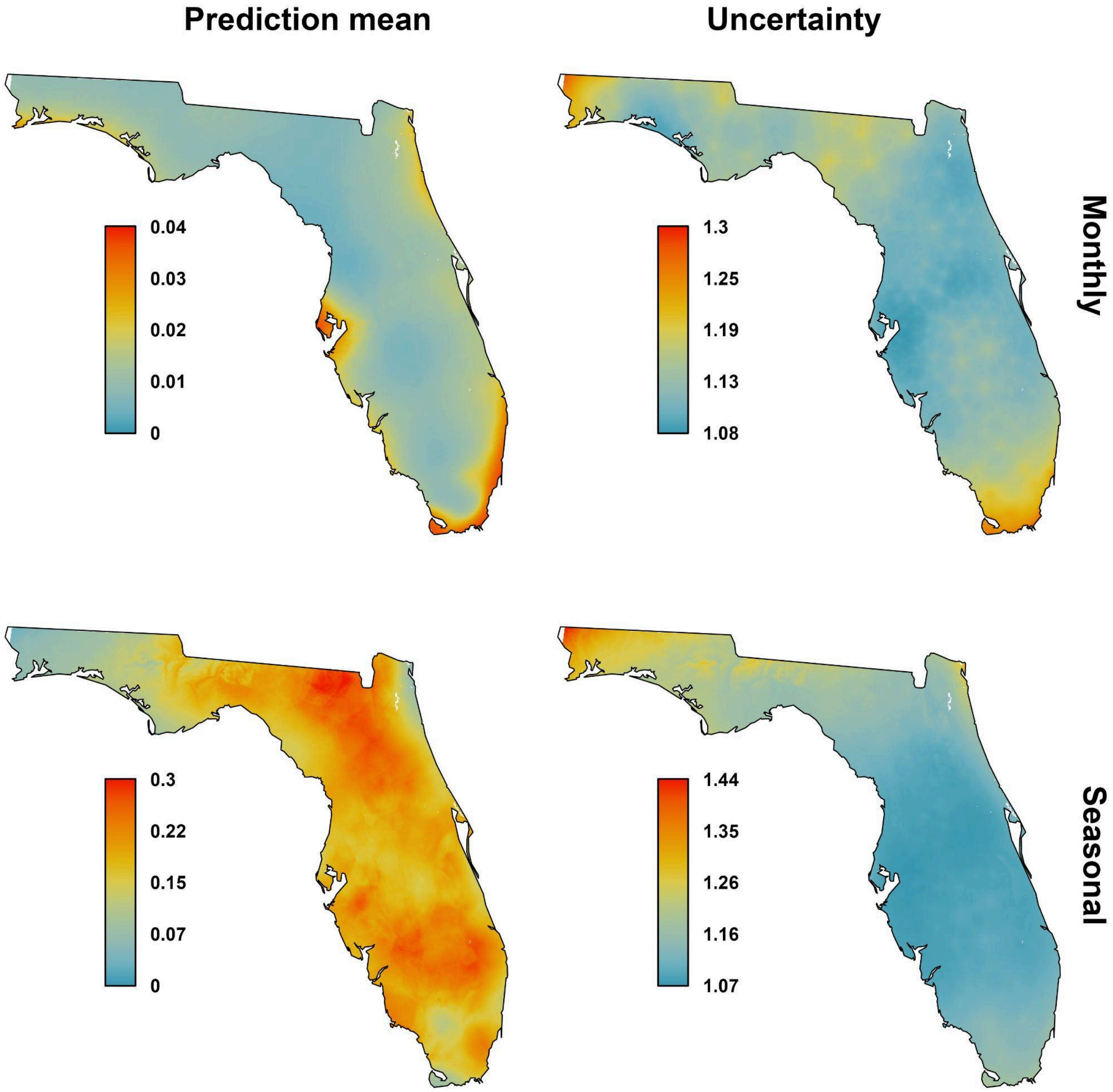

Fig. 5. Summary of state-wide prediction means and associated uncertainty of West Nile Virus seropositive counts during the years of 2001 – 2019 in the Florida sentinel chicken system. Predictions were obtained from spatiotemporal models fitted to data aggregated to both seasonal (top panels) and monthly (bottom panels) temporal scales of the WNV activity season (June – December). Predictions are mapped using a 99.9th percentile quantile truncation for visualization.

References:

Amdouni, J., Monaco, F., Portanti, O., Sghaier, S., Conte, A., Hassine, T. B., Polci, A., Valleriani, F., Gennaro, A. D., Zoueri, M., Savini, G., & Hammami, S. (2020). Detection of enzootic circulation of a new strain of West Nile virus lineage 1 in sentinel chickens in the north of Tunisia. *Acta Tropica*, *202*, 105223. https://doi.org/10.1016/j.actatropica.2019.105223

Anderson, S. C., Ward, E. J., English, P. A., Barnett, L. A. K., & Thorson, J. T. (2024). *sdmTMB: An R Package for Fast, Flexible, and User-Friendly Generalized Linear Mixed Effects Models with Spatial and Spatiotemporal Random Fields* (p. 2022.03.24.485545). bioRxiv. https://doi.org/10.1101/2022.03.24.485545

Bakka, H., Rue, H., Fuglstad, G.-A., Riebler, A., Bolin, D., Krainski, E., Simpson, D., & Lindgren, F. (2018). *Spatial modelling with R-INLA: A review* (No. arXiv:1802.06350). arXiv. https://doi.org/10.48550/arXiv.1802.06350

Barker, C. M. (2019). Models and Surveillance Systems to Detect and Predict West Nile Virus Outbreaks. *Journal of Medical Entomology*, *56*(6), 1508–1515. https://doi.org/10.1093/jme/tjz150

Bauer, A. M., Guralnick, R. P., Whitehead, S. A., Barve, N., Allen, J. M., & Campbell, L. P. (2024). Land use predicts proportion of West Nile virus vector-competent mosquitoes. *Ecosphere*, *15*(2), e4771. https://doi.org/10.1002/ecs2.4771

Beeman, S. P., Downs, J. A., Unnasch, T. R., & Unnasch, R. S. (2022). *West Nile Virus and Eastern Equine Encephalitis Virus High Probability Habitat Identification for the Selection of Sentinel Chicken Surveillance Sites in Florida*. https://doi.org/10.2987/21-7049

Beeman, S. P., Morrison, A. M., Unnasch, T. R., & Unnasch, R. S. (2021). Ensemble ecological niche modeling of West Nile virus probability in Florida. *PLOS ONE*, *16*(10), e0256868. https://doi.org/10.1371/journal.pone.0256868

Bocinsky, R. K., Beaudette, D., Chamberlain, S., Hollister, J., & Gustavsen, J. (2025). *FedData: Download Geospatial Data Available from Several Federated Data Sources* (Version 4.3.0) [Computer software]. https://cran.r-project.org/web/packages/FedData/index.html

Bowden, S. E., Magori, K., & Drake, J. M. (2011). Regional differences in the association between land cover and West Nile virus disease incidence in humans in the United States. *The American Journal of Tropical Medicine and Hygiene*, *84*(2), 234–238. https://doi.org/10.4269/ajtmh.2011.10-0134

Brooks, M., Bolker, B., Kristensen, K., Maechler, M., Magnusson, A., McGillycuddy, M., Skaug, H., Nielsen, A., Berg, C., Bentham, K. van, Sadat, N., Lüdecke, D., Lenth, R., O'Brien, J., Geyer, C. J., Jagan, M., Wiernik, B., Stouffer, D. B., Agronah, M., & Akdur, H. T. K. (2025). *glmmTMB: Generalized Linear Mixed Models using Template Model Builder* (Version 1.1.11) [Computer software]. https://cran.r-project.org/web/packages/glmmTMB/index.html

Brown, L., Medlock, J., & Murray, V. (2014). Impact of drought on vector-borne diseases – how does one manage the risk? *Public Health*, *128*(1), 29–37. https://doi.org/10.1016/j.puhe.2013.09.006

Brüssow, H., & Figuerola, J. (2025). The Spread of the Mosquito-Transmitted West Nile Virus in North America and Europe. *Microbial Biotechnology*, *18*(3), e70120. https://doi.org/10.1111/1751-7915.70120

Campbell, G. L., Marfin, A. A., Lanciotti, R. S., & Gubler, D. J. (2002). West Nile virus. *The Lancet Infectious Diseases*, *2*(9), 519–529.

https://doi.org/10.1016/S1473-3099(02)00368-7

Campbell, L. P., Guralnick, R. P., Giordano, B. V., Sallam, M. F., Bauer, A. M., Tavares, Y., Allen, J. M., Efstathion, C., Bartlett, S., Wishard, R., Xue, R.-D., Allen, B., Tressler, M., Qualls, W., & Burkett-Cadena, N. D. (2022). Spatiotemporal Modeling of Zoonotic Arbovirus Transmission in Northeastern Florida Using Sentinel Chicken Surveillance and Earth Observation Data. *Remote Sensing*, *14*(14), Article 14. https://doi.org/10.3390/rs14143388

CDC. (2024, May 17). *West Nile Virus*. West Nile Virus. https://www.cdc.gov/west-nile-virus/index.html

Cherry, B., Trock, S. C., Glaser, A., Kramer, L., Ebel, G. D., Glaser, C., & Miller, J. R. (2001). Sentinel Chickens as a Surveillance Tool for West Nile Virus in New York City, 2000. *Annals of the New York Academy of Sciences*, *951*(1), 343–346. https://doi.org/10.1111/j.1749-6632.2001.tb02714.x

Chung, W. M., Buseman, C. M., Joyner, S. N., Hughes, S. M., Fomby, T. B., Luby, J. P., & Haley, R. W. (2013). The 2012 West Nile Encephalitis Epidemic in Dallas, Texas. *JAMA*, *310*(3), 297. https://doi.org/10.1001/jama.2013.8267

Ciota, A. T. (2017). West Nile virus and its vectors. *Current Opinion in Insect Science*, *22*, 28–36. https://doi.org/10.1016/j.cois.2017.05.002

Crowder, D. W., Dykstra, E. A., Brauner, J. M., Duffy, A., Reed, C., Martin, E., Peterson, W., Carrière, Y., Dutilleul, P., & Owen, J. P. (2013). West Nile Virus Prevalence across Landscapes Is Mediated by Local Effects of Agriculture on Vector and Host Communities. *PLOS ONE*, *8*(1), e55006. https://doi.org/10.1371/journal.pone.0055006

Czernecki, B., Głogowski, A., Nowosad, J., & data), I.-P. (source of the. (2025). *climate:*

Interface to Download Meteorological (and Hydrological) Datasets (Version 1.2.3) [Computer software]. https://cran.r-project.org/web/packages/climate/index.html

Dahlin, K. J.-M., O'Regan, S. M., Han, B. A., Schmidt, J. P., & Drake, J. M. (2024). Impacts of host availability and temperature on mosquito-borne parasite transmission. *Ecological Monographs*, *94*(2), e1603. https://doi.org/10.1002/ecm.1603

Day, J. F., Tabachnick, W. J., & Smartt, C. T. (2015). Factors That Influence the Transmission of West Nile Virus in Florida. *Journal of Medical Entomology*, *52*(5), 743–754. https://doi.org/10.1093/jme/tjv076

DeGroote, J. P., Sugumaran, R., & Ecker, M. (2014). Landscape, demographic and climatic associations with human West Nile virus occurrence regionally in 2012 in the United States of America. *Geospatial Health*, *9*(1), 153–168. https://doi.org/10.4081/gh.2014.13

Dewitz, J. (2024). *National Land Cover Database (NLCD)* (Version 3.0) [Dataset]. U.S. Geological Survey. https://doi.org/10.5066/P9KZCM54

Diggle, P. J., & Gabriel, E. (2010). Spatio-temporal point processes. In A. Gelfand, P. J. Diggle, M. Fuentes, & P. Guttorp (Eds.), *Handbook of Spatial Statistics* (pp. 449–461). CRC Press. http://www.crcpress.com/product/isbn/9781420072877

Dye-Braumuller, K. C., Gordon, J. R., McCoy, K., Johnson, D., Dinglasan, R., & Nolan, M. S. (2022). Riding the Wave: Reactive Vector-Borne Disease Policy Renders the United States Vulnerable to Outbreaks and Insecticide Resistance. *Journal of Medical Entomology*, *59*(2), 401–411. https://doi.org/10.1093/jme/tjab219

Eisen, L., Barker, C. M., Moore, C. G., Pape, W. J., Winters, A. M., & Cheronis, N. (2010). Irrigated agriculture is an important risk factor for West Nile virus disease in the hyperendemic Larimer-Boulder-Weld area of north central Colorado. *Journal of Medical*

Entomology, *47*(5), 939–951. https://doi.org/10.1603/me10036

Ezenwa, V. O., Milheim, L. E., Coffey, M. F., Godsey, M. S., King, R. J., & Guptill, S. C. (2007). Land cover variation and West Nile virus prevalence: Patterns, processes, and implications for disease control. *Vector Borne and Zoonotic Diseases (Larchmont, N.Y.)*, *7*(2), 173–180. https://doi.org/10.1089/vbz.2006.0584

FDOH. (2025). Non-Human Mosquito-Borne Disease Monitoring Activities. In *Mosquito-Borne Disease Guidebook*. 2022. https://www.floridahealth.gov/diseases-and-conditions/mosquito-borne-diseases/_documents/guidebook-chapter-ten.pdf

Fox, J., & Weisberg, S. (2018). *An R Companion to Applied Regression* (3rd ed.). https://us.sagepub.com/en-us/nam/an-r-companion-to-applied-regression/book246125

Garabed, R. B., Jolles, A., Garira, W., Lanzas, C., Gutierrez, J., & Rempala, G. (2020). Multi-scale dynamics of infectious diseases. *Interface Focus*, *10*(1), 20190118. https://doi.org/10.1098/rsfs.2019.0118

Gardner, A. M., Hamer, G. L., Hines, A. M., Newman, C. M., Walker, E. D., & Ruiz, M. O. (2012). Weather Variability Affects Abundance of Larval Culex (Diptera: Culicidae) in Storm Water Catch Basins in Suburban Chicago. *Journal of Medical Entomology*, *49*(2), 270–276. https://doi.org/10.1603/ME11073

Gelfand, A. E., & Banerjee, S. (2017). Bayesian Modeling and Analysis of Geostatistical Data. *Annual Review of Statistics and Its Application*, *4*(Volume 4, 2017), 245–266. https://doi.org/10.1146/annurev-statistics-060116-054155

Gilbert, N., & Raworth, D. A. (1996). Forum: Insects And Temperature—A General Theory. *The Canadian Entomologist*, *128*(1), 1–13. https://doi.org/10.4039/Ent1281-1

Gleiser, R. M., Mackay, A. J., Roy, A., Yates, M. M., Vaeth, R. H., Faget, G. M., Folsom, A. E., Augustine, W. F., Wells, R. A., & Perich, M. J. (2007). West Nile Virus surveillance in East Baton Rouge Parish, Louisiana. *Journal of the American Mosquito Control Association*, *23*(1), 29–36. https://doi.org/10.2987/8756-971X(2007)23[29:WNVSIE]2.0.CO;2

Ham, K. (2013). OpenRefine (version 2.5). Http://openrefine.org. Free, open-source tool for cleaning and transforming data. *Journal of the Medical Library Association : JMLA*, *101*(3), 233–234. https://doi.org/10.3163/1536-5050.101.3.020

Harp, R. D., Holcomb, K. M., Retkute, R., Prusokiene, A., Prusokas, A., Ertem, Z., Ajelli, M., Kummer, A. G., Litvinova, M., Merler, S., Piontti, A. P. y., Poletti, P., Vespignani, A., Wilke, A. B. B., Zardini, A., Smith, K. H., Armstrong, P., DeFelice, N., Keyel, A., … Johansson, M. A. (2025). Evaluation of the 2022 West Nile virus forecasting challenge, USA. *Parasites & Vectors*, *18*(1), 152. https://doi.org/10.1186/s13071-025-06767-2

Hartig, F. (2025). *DHARMa: Residual Diagnostics for Hierarchical (Multi-Level / Mixed) Regression Models* [R]. https://github.com/florianhartig/DHARMa

Hebert, N. E., Sameoto, J. A., Keith, D. M., Barrett, M. A., Brown, C. J., & Mills Flemming, J. (2024). Comparing spatiotemporal species distribution models: A case study of a Scotian Shelf sea cucumber (Cucumaria frondosa). *Ecosphere*, *15*(4), e4822. https://doi.org/10.1002/ecs2.4822

Hijmans, R. J. (2025). *terra: Spatial Data Analysis* (Version 1.8-46) [C++]. rspatial. https://github.com/rspatial/terra (Original work published 2018)

Holcomb, K. M., Mathis, S., Staples, J. E., Fischer, M., Barker, C. M., Beard, C. B., Nett, R. J., Keyel, A. C., Marcantonio, M., Childs, M. L., Gorris, M. E., Rochlin, I., Hamins-Puértolas, M., Ray, E. L., Uelmen, J. A., DeFelice, N., Freedman, A. S., Hollingsworth, B. D., Das, P., … Johansson, M. A. (2023). Evaluation of an open forecasting challenge to assess skill of West Nile virus neuroinvasive disease prediction. *Parasites & Vectors*, *16*(1), 11. https://doi.org/10.1186/s13071-022-05630-y

Ives, A. R. (2022). Random errors are neither: On the interpretation of correlated data. *Methods in Ecology and Evolution*, *13*(10), 2092–2105. https://doi.org/10.1111/2041-210X.13971

Johnson, B. J., Munafo, K., Shappell, L., Tsipoura, N., Robson, M., Ehrenfeld, J., & Sukhdeo, M. V. K. (2012). The roles of mosquito and bird communities on the prevalence of West Nile virus in urban wetland and residential habitats. *Urban Ecosystems*, *15*(3), 513–531. https://doi.org/10.1007/s11252-012-0248-1

Kain, M. P., & Bolker, B. M. (2019). Predicting West Nile virus transmission in North American bird communities using phylogenetic mixed effects models and eBird citizen science data. *Parasites & Vectors*, *12*(1), 395. https://doi.org/10.1186/s13071-019-3656-8

Keyel, A. C., Gorris, M. E., Rochlin, I., Uelmen, J. A., Chaves, L. F., Hamer, G. L., Moise, I. K., Shocket, M., Kilpatrick, A. M., DeFelice, N. B., Davis, J. K., Little, E., Irwin, P., Tyre, A. J., Helm Smith, K., Fredregill, C. L., Elison Timm, O., Holcomb, K. M., Wimberly, M. C., … Smith, R. L. (2021). A proposed framework for the development and qualitative evaluation of West Nile virus models and their application to local public health decision-making. *PLoS Neglected Tropical Diseases*, *15*(9), e0009653. https://doi.org/10.1371/journal.pntd.0009653

Kiryluk, H. D., Beard, C. B., & Holcomb, K. M. (2024). The use of environmental data in descriptive and predictive models of vector-borne disease in North America. *Journal of Medical Entomology*, *61*(3), 595–602. https://doi.org/10.1093/jme/tjae031

Koch, R. T., Erazo, D., Folly, A. J., Johnson, N., Dellicour, S., Grubaugh, N. D., & Vogels, C. B. F. (2024). Genomic epidemiology of West Nile virus in Europe. *One Health*, *18*, 100664. https://doi.org/10.1016/j.onehlt.2023.100664

Koenraadt, C. J. M., & Harrington, L. C. (2008). Flushing Effect of Rain on Container-Inhabiting Mosquitoes Aedes aegypti and Culex pipiens (Diptera: Culicidae). *Journal of Medical Entomology*, *45*(1), 28–35. https://doi.org/10.1093/jmedent/45.1.28

Krainski, E., Gómez-Rubio, V., Bakka, H., Lenzi, A., Castro-Camilo, D., Simpson, D., Lindgren, F., & Rue, H. (2018). *Advanced Spatial Modeling with Stochastic Partial Differential Equations Using R and INLA*. Chapman and Hall/CRC. https://doi.org/10.1201/9780429031892

Kwan, J. L., Kluh, S., Madon, M. B., Nguyen, D. V., Barker, C. M., & Reisen, W. K. (2010). Sentinel Chicken Seroconversions Track Tangential Transmission of West Nile Virus to Humans in the Greater Los Angeles Area of California. *The American Journal of Tropical Medicine and Hygiene*, *83*(5), 1137–1145. https://doi.org/10.4269/ajtmh.2010.10-0078

Kwan, J. L., Park, B. K., Carpenter, T. E., Ngo, V., Civen, R., & Reisen, W. K. (2012). Comparison of Enzootic Risk Measures for Predicting West Nile Disease, Los Angeles, California, USA, 2004–2010. *Emerging Infectious Diseases*, *18*(8), 1298–1306. https://doi.org/10.3201/eid1808.111558

Kyriakidis, P. C., & Journel, A. G. (1999). Geostatistical Space–Time Models: A Review. *Mathematical Geology*, *31*(6), 651–684. https://doi.org/10.1023/A:1007528426688

Lauer, S. A., Brown, A. C., & Reich, N. G. (2020). Infectious Disease Forecasting for Public Health. In *Population Biology of Vector-Borne Diseases*. Oxford University Press.

http://arxiv.org/abs/2006.00073

Lindgren, F. (2025). *fmesher: Triangle Meshes and Related Geometry Tools* (p. 0.3.0) [Computer software]. https://CRAN.R-project.org/package=fmesher

Lindgren, F., Bakka, H., Bolin, D., Krainski, E., & Rue, H. (2023). *A diffusion-based spatio-temporal extension of Gaussian Matérn fields* (No. arXiv:2006.04917). arXiv. https://doi.org/10.48550/arXiv.2006.04917

Lindgren, F., Rue, H., & Lindström, J. (2011). An Explicit Link between Gaussian Fields and Gaussian Markov Random Fields: The Stochastic Partial Differential Equation Approach. *Journal of the Royal Statistical Society Series B: Statistical Methodology*, *73*(4), 423–498. https://doi.org/10.1111/j.1467-9868.2011.00777.x

Lüdecke, D., Ben-Shachar, M. S., Patil, I., Waggoner, P., & Makowski, D. (2021). performance: An R Package for Assessment, Comparison and Testing of Statistical Models. *Journal of Open Source Software*, *6*(60), 3139. https://doi.org/10.21105/joss.03139

Magurran, A. E., Baillie, S. R., Buckland, S. T., Dick, J. M., Elston, D. A., Scott, E. M., Smith, R. I., Somerfield, P. J., & Watt, A. D. (2010). Long-term datasets in biodiversity research and monitoring: Assessing change in ecological communities through time. *Trends in Ecology & Evolution*, *25*(10), 574–582. https://doi.org/10.1016/j.tree.2010.06.016

Marm Kilpatrick, A., Daszak, P., Jones, M. J., Marra, P. P., & Kramer, L. D. (2006). Host heterogeneity dominates West Nile virus transmission. *Proceedings of the Royal Society B: Biological Sciences*, *273*(1599), 2327–2333. https://doi.org/10.1098/rspb.2006.3575

McCarter, M. S. J., Self, S., Dye-Braumuller, K. C., Lee, C., Li, H., & Nolan, M. S. (2023). The utility of a Bayesian predictive model to forecast neuroinvasive West Nile virus disease in the United States of America, 2022. *PLOS ONE*, *18*(9), e0290873.

https://doi.org/10.1371/journal.pone.0290873

McGuinness, S. L., Lau, C. L., & Leder, K. (2023). The evolving Japanese encephalitis situation in Australia and implications for travel medicine. *Journal of Travel Medicine*, *30*(2), taad029. https://doi.org/10.1093/jtm/taad029

McNulty, S. G., Hoffman, J. S., Brown, C., Dello, K. D., Knox, P. N., Lascurain, A., Mickalonis, C., Mitchum, G. T., Iii, L. R., Schaefer, M., Smith, G. P., Camp, J. S., & Wood, K. M. (2023). Southeast. In *Fifth National Climate Assessment*. U.S. Global Change Research Program, Washington, DC. https://nca2023.globalchange.gov/chapter/22/

Molina-Guzmán, L. P., Gutiérrez-Builes, L. A., & Ríos-Osorio, L. A. (2022). Models of spatial analysis for vector-borne diseases studies: A systematic review. *Veterinary World*, *15*(8), 1975–1989. https://doi.org/10.14202/vetworld.2022.1975-1989

Mordecai, E. A., Caldwell, J. M., Grossman, M. K., Lippi, C. A., Johnson, L. R., Neira, M., Rohr, J. R., Ryan, S. J., Savage, V., Shocket, M. S., Sippy, R., Stewart Ibarra, A. M., Thomas, M. B., & Villena, O. (2019). Thermal biology of mosquito-borne disease. *Ecology Letters*, *22*(10), 1690–1708. https://doi.org/10.1111/ele.13335

Myer, M. H., Campbell, S. R., & Johnston, J. M. (2017). Spatiotemporal modeling of ecological and sociological predictors of West Nile virus in Suffolk County, NY, mosquitoes. *Ecosphere*, *8*(6), e01854. https://doi.org/10.1002/ecs2.1854

Myer, M. H., & Johnston, J. M. (2019). Spatiotemporal Bayesian modeling of West Nile virus: Identifying risk of infection in mosquitoes with local-scale predictors. *Science of The Total Environment*, *650*, 2818–2829. https://doi.org/10.1016/j.scitotenv.2018.09.397

NOAA. (2016). *Land Cover Change*. https://coast.noaa.gov/states/fast-facts/land-cover-change.html

Nosrat, C., Altamirano, J., Anyamba, A., Caldwell, J. M., Damoah, R., Mutuku, F., Ndenga, B., & LaBeaud, A. D. (2021). Impact of recent climate extremes on mosquito-borne disease transmission in Kenya. *PLoS Neglected Tropical Diseases*, *15*(3), e0009182. https://doi.org/10.1371/journal.pntd.0009182

Oyafuso, Z. S., Barnett, L. A. K., & Kotwicki, S. (2021). Incorporating spatiotemporal variability in multispecies survey design optimization addresses trade-offs in uncertainty. *ICES Journal of Marine Science*, *78*(4), 1288–1300. https://doi.org/10.1093/icesjms/fsab038

Pavlovskiĭ, E. N. (1966). *Natural nidality of transmissible diseases, with special reference to the landscape epidemiology of zooanthroponoses*. University of Illinois Press.

Pebesma, E., & Bivand, R. (2023). *Spatial Data Science: With Applications in R*. Chapman and Hall/CRC. https://doi.org/10.1201/9780429459016

Poh, K. C., Chaves, L. F., Reyna-Nava, M., Roberts, C. M., Fredregill, C., Bueno, R., Debboun, M., & Hamer, G. L. (2019). The influence of weather and weather variability on mosquito abundance and infection with West Nile virus in Harris County, Texas, USA. *Science of The Total Environment*, *675*, 260–272. https://doi.org/10.1016/j.scitotenv.2019.04.109

R Core Team. (2025). *R: A language and environment for statistical computing* [R]. R Foundation for Statistical Computing. https://www.R-project.org/

Rees, E. M., Minter, A., Edmunds, W. J., Lau, C. L., Kucharski, A. J., & Lowe, R. (2021). Transmission modelling of environmentally persistent zoonotic diseases: A systematic review. *The Lancet Planetary Health*, *5*(7), e466–e478. https://doi.org/10.1016/S2542-5196(21)00137-6

Reich, B. J., Yang, S., Guan, Y., Giffin, A. B., Miller, M. J., & Rappold, A. (2021). A Review of Spatial Causal Inference Methods for Environmental and Epidemiological Applications. *International Statistical Review*, *89*(3), 605–634. https://doi.org/10.1111/insr.12452

Reisen, W. K. (2013). Ecology of West Nile virus in North America. *Viruses*, *5*(9), 2079–2105. https://doi.org/10.3390/v5092079

Roberts, M., Dobson, A., Restif, O., & Wells, K. (2021). Challenges in modelling the dynamics of infectious diseases at the wildlife–human interface. *Epidemics*, *37*, 100523. https://doi.org/10.1016/j.epidem.2021.100523

Rochlin, I., Faraji, A., Healy, K., & Andreadis, T. G. (2019). West Nile Virus Mosquito Vectors in North America. *Journal of Medical Entomology*, *56*(6), 1475–1490. https://doi.org/10.1093/jme/tjz146

Rue, H., & Held, L. (2005). *Gaussian Markov Random Fields: Theory and Applications*. Chapman & Hall/CRC.

Rue, H., Lindgren, F., van Niekerk, J., & Krainski, E. (2025). *R-INLA Project*. https://www.r-inla.org/home

Rue, H., Martino, S., & Chopin, N. (2009). Approximate Bayesian inference for latent Gaussian models by using integrated nested Laplace approximations. *Journal of the Royal Statistical Society: Series B (Statistical Methodology)*, *71*(2), 319–392. https://doi.org/10.1111/j.1467-9868.2008.00700.x

Ruiz, M. O., Walker, E. D., Foster, E. S., Haramis, L. D., & Kitron, U. D. (2007). Association of West Nile virus illness and urban landscapes in Chicago and Detroit. *International Journal of Health Geographics*, *6*(1), 10. https://doi.org/10.1186/1476-072X-6-10

Sallam, M. F., Xue, R.-D., Pereira, R. M., & Koehler, P. G. (2016). Ecological niche modeling of mosquito vectors of West Nile virus in St. John's County, Florida, USA. *Parasites & Vectors*, *9*(1), 371. https://doi.org/10.1186/s13071-016-1646-7

Schumacher, A. E., Kyu, H. H., Aali, A., Abbafati, C., Abbas, J., Abbasgholizadeh, R., Abbasi, M. A., Abbasian, M., ElHafeez, S. A., Abdelmasseh, M., Abd-Elsalam, S., Abdelwahab, A., Abdollahi, M., Abdoun, M., Abdullahi, A., Abdurehman, A. M., Abebe, M., Abedi, A., Abedi, A., … Murray, C. J. L. (2024). Global age-sex-specific mortality, life expectancy, and population estimates in 204 countries and territories and 811 subnational locations, 1950–2021, and the impact of the COVID-19 pandemic: A comprehensive demographic analysis for the Global Burden of Disease Study 2021. *The Lancet*, *403*(10440), 1989–2056. https://doi.org/10.1016/S0140-6736(24)00476-8

Shaman, J., Day, J. F., & Stieglitz, M. (2005). Drought-Induced Amplification and Epidemic Transmission of West Nile Virus in Southern Florida. *Journal of Medical Entomology*, *42*(2), 134–141. https://doi.org/10.1093/jmedent/42.2.134

Solà, O., Kéry, M., Aquilué, N., & Brotons, L. (2025). Sampling effort required for fitting spatially explicit models of species distribution dynamics. *Ecological Modelling*, *501*, 110998. https://doi.org/10.1016/j.ecolmodel.2024.110998

Streng, K., Atama ,Nnomzie, Chandler ,Felicity, Blom ,Rody, van der Jeugd ,Henk, Schrama ,Maarten, Koopmans ,Marion P.G., van der Poel ,Wim H.M., & and Sikkema, R. S. (2024). Sentinel chicken surveillance reveals previously undetected circulation of West Nile virus in the Netherlands. *Emerging Microbes & Infections*, *13*(1), 2406278. https://doi.org/10.1080/22221751.2024.2406278

Tavares, Y., Day, J., Giordano, B. V., Eastmond, B., Burkett-Cadena, N., Guralnick, R. P., Martin, E., & Campbell, L. P. (2024). Regional variation in the landscape ecology of

West Nile virus sentinel chicken seroconversion in Florida. *PloS One*, *19*(10), e0305510. https://doi.org/10.1371/journal.pone.0305510

Thornton, M. M., Shrestha, R., Wei, Y., Thornton, P. E., & Kao, S.-C. (2022). *Daymet: Daily Surface Weather Data on a 1-km Grid for North America, Version 4 R1* [Dataset]. https://doi.org/10.3334/ORNLDAAC/2129

Thorson, J., & Kristensen, K. (2024). *Spatio-Temporal Models for Ecologists* (1st ed.). Chapman and Hall/CRC. https://doi.org/10.1201/9781003410294

Thorson, J. T., Anderson, S. C., Goddard, P., & Rooper, C. N. (2025). tinyVAST: R Package With an Expressive Interface to Specify Lagged and Simultaneous Effects in Multivariate Spatio-Temporal Models. *Global Ecology and Biogeography*, *34*(4), e70035. https://doi.org/10.1111/geb.70035

Thorson, J. T., & Kristensen, K. (2016). Implementing a generic method for bias correction in statistical models using random effects, with spatial and population dynamics examples. *Fisheries Research*, *175*, 66–74. https://doi.org/10.1016/j.fishres.2015.11.016

Thorson, J. T., Skaug, H. J., Kristensen, K., Shelton, A. O., Ward, E. J., Harms, J. H., & Benante, J. A. (2015). The importance of spatial models for estimating the strength of density dependence. *Ecology*, *96*(5), 1202–1212. https://doi.org/10.1890/14-0739.1

Vilibic-Cavlek, T., Petrovic, T., Savic, V., Barbic, L., Tabain, I., Stevanovic, V., Klobucar, A., Mrzljak, A., Ilic, M., Bogdanic, M., Benvin, I., Santini, M., Capak, K., Monaco, F., Listes, E., & Savini, G. (2020). Epidemiology of Usutu Virus: The European Scenario. *Pathogens*, *9*(9), 699. https://doi.org/10.3390/pathogens9090699

Voeten, C. C. (2023). *buildmer: Stepwise Elimination and Term Reordering for Mixed-Effects Regression* (Version 2.11) [Computer software].

https://cran.r-project.org/web/packages/buildmer/index.html

Wang, Y., Chen, X., & Xue, F. (2024). A Review of Bayesian Spatiotemporal Models in Spatial Epidemiology. *ISPRS International Journal of Geo-Information*, *13*(3), Article 3. https://doi.org/10.3390/ijgi13030097

Ward, M. J., Sorek-Hamer, M., Henke, J. A., Little, E., Patel, A., Shaman, J., Vemuri, K., & DeFelice, N. B. (2023). A Spatially Resolved and Environmentally Informed Forecast Model of West Nile Virus in Coachella Valley, California. *GeoHealth*, *7*(12), e2023GH000855. https://doi.org/10.1029/2023GH000855

Wen, T.-H., Lin, M.-H., Teng, H.-J., & Chang, N.-T. (2015). Incorporating the human-*Aedes* mosquito interactions into measuring the spatial risk of urban dengue fever. *Applied Geography*, *62*, 256–266. https://doi.org/10.1016/j.apgeog.2015.05.003

WHO. (2025). *World Health Organization Fact Sheet. Vector-borne Diseases.* [Database]. World Health Organization Fact Sheet. Vector-Borne Diseases. https://www.who.int/news-room/fact-sheets/detail/vector-borne-diseases

Wickham, H., Averick, M., Bryan, J., Chang, W., McGowan, L. D., François, R., Grolemund, G., Hayes, A., Henry, L., Hester, J., Kuhn, M., Pedersen, T. L., Miller, E., Bache, S. M., Müller, K., Ooms, J., Robinson, D., Seidel, D. P., Spinu, V., … Yutani, H. (2019). Welcome to the Tidyverse. *Journal of Open Source Software*, *4*(43), 1686. https://doi.org/10.21105/joss.01686

Wikle, C. K., Zammit-Mangion, A., & Cressie, N. A. C. (2019). *Spatio-temporal statistics with R*. CRC Press, Taylor and Francis Group.

Wimberly, M. C., Davis, J. K., Hildreth, M. B., & Clayton, J. L. (2022). Integrated Forecasts Based on Public Health Surveillance and Meteorological Data Predict West Nile Virus in a High-Risk Region of North America. *Environmental Health Perspectives*, *130*(8), 087006. https://doi.org/10.1289/EHP10287

Wimberly, M. C., Lamsal, A., Giacomo, P., & Chuang, T.-W. (2014). *Regional Variation of Climatic Influences on West Nile Virus Outbreaks in the United States*. https://doi.org/10.4269/ajtmh.14-0239

Zheng, N., Cadigan, N., & Thorson, J. T. (2024). *A note on numerical evaluation of conditional Akaike information for nonlinear mixed-effects models* (No. arXiv:2411.14185). arXiv. https://doi.org/10.48550/arXiv.2411.14185

SUPPLEMENTAL INFORMATION FOR:

Baecher, JA, AV Anand, AM Bauer, YSanchez, J Thorson, RP Guralnick, LP Campbell. Spatiotemporal Dynamics of West Nile Virus Seroconversion: Insights from Two Decades of Monitoring in Florida. *Science of the Total Environment* (submitted).

1. Data preparation

2.1. Land use land cover:

For this analysis, the following land use land cover classes were extracted: (i) “developed” (NLCD classes: 21 – 24), (ii) “natural” (classes: 41 – 43, 52, and 71 – 72), and (iv) “wetlands” (classes: 90 and 95).

2. Statistical analysis

2.1. Variable selection:

This study included three climate variables (max temperature, min temperature, and cumulative precipitation) and three land cover variables (proportions developed, natural, and wetlands). For each climate variable, a one- and two- timestep lag was calculated, resulting in nine candidate climate variables. In the candidate set of univariate models, both linear and quadratic parameterizations were included, yielding a total of 25 seasonal and monthly models (including an intercept-only model). Examination of the effect sizes of each of these predictions reduced the initial candidate set to 22 models for the seasonal timescale and 18 models for the monthly timescales. Next backwards model selection was used to create a multi-variable model. Finally, this model was reduced based on multicollinearity (VIF > 5), removing three variables from the seasonal model (tmax_lag1^2, tmin^2, tmin_lag1^2), yielding a final set of four predictors for both the monthly and seasonal spatiotemporal models:

Monthly model predictors:

- Maximum temperature^2
- Minimum temperature at 1-month lag^2
- Cumulative precipitation^2
- Proportion developed land^2

Seasonal model predictors:

- Maximum temperature at 1-year lag^2
- Minimum temperature at 1-year lag^2
- Cumulative precipitation^2
- Cumulative precipitation at 6-month lag

2.2. Epsilon bias-correction estimator:

Methods for obtaining derived quantities from mixed-models often require calculating non-linear functions of both fixed and random effects. In the case of a mixed-model fitted using a log-link function, predictions across levels of a random effect would be obtained by calculating an exponential inversion function; a function which transforms both mean and variance of those values, introducing significant bias that could unduly influence model interpretation.

This method yields unbiased estimates by sampling from the models random effects while holding fixed effects at their maximum likelihood estimate (see Eq. 1). To provide a brief overview of this estimator, we can first examine the non-linear calculation of derived quantities. To begin, the Laplace approximation of the joint log-likelihood of a mixed-model with both fixed θ and random effects u, given the data x, is represented as $\ell(\theta, u; x)$, with the marginal likelihood being $\boldsymbol{\mathcal{L}}(\theta; x) = \int exp(f(\theta, u; x)du$. To apply the epsilon bias-correction estimator, we include an additional term ε ("epsilon") to compute an augmented likelihood $\boldsymbol{\mathcal{L}}^*(\theta, \varepsilon; x)$:

$$\ell^*(\theta, u, \varepsilon; x) = \ell(\theta, u; x) - \varepsilon\, \phi(\theta,\ u), \qquad \text{(Eq. 1a)}$$

$$\boldsymbol{\mathcal{L}}^*(\theta, \varepsilon; x) = \int exp(\ell(\theta, u, \varepsilon; x))\ du. \qquad \text{(Eq. 1b)}$$

To calculate the desired unbiased estimator ϕ we calculate the following partial differential equation with respect to at ε, evaluated at $\varepsilon = 0$:

$$\mathbb{E}[\phi(\theta,\ u)] = \frac{\partial}{\partial\varepsilon} log(\boldsymbol{\mathcal{L}}^*(\theta, \varepsilon; x)) \mid \varepsilon = 0, \qquad \text{(Eq. 1c)}$$

where, $\mathbb{E}[\phi(\theta,\ u)]$ is the expected mean value of the desired unbiased estimate ϕ given the data $\boldsymbol{x}$. This method provides a high-quality estimator of ϕ, which corrects for both non-linearity and skewness of fixed effects in the the commonly used "plug-in" estimator prior ($\mathbb{E}[\phi(u)]$).

In practice, the epsilon method was used to obtain derived quantities of total WNV seroconversion by first taking 500 Multivariate Normal (MVN) samples from the inner Hessian matrix, using the full training dataset, and then adjusted using the *sdmTMB* package's function *get_index*. Therefore, the 95% confidence intervals around these predictions reflect the cumulative variation of the full spatiotemporal range of training set data. Due to computational intensity, the epsilon method was not applied to estimate state-wide predictions (i.e., Fig. 3 – 5 in the main text). Alternatively, to project models' predictions to the state-wide level, the *sdmTMB*'s function *simulate* was used to take 100 MVN samples were taken to calculate predictions from the joint prediction matrix at each pixel across all timesteps—constituting >19.5-million pixel predictions for monthly models and >2.7-million pixel predictions for seasonal data.

Supplemental Information Tables:

SI Table 1. Description of the model components leading to the development of Gaussian Markov random field GLMM models, including degrees of freedom (“DF”), effective degrees of freedom (“EDF”), conditional percent deviance explained (“CPDE”), and marginal AIC. Models were fitted at both seasonal and monthly time scales. These models are described in terms of their major components, including intercepts (“~1”), fixed effects, random effects, and Gaussian Markov random fields (GMRF).

Model components	**DF**	**EDF**		**CPDE**	**Marginal AIC**	
	FE	RE	GMRF		Δ	ω
Seasonal						
WNV ~ Fixed effects + Random effects + GMRF		304.65	231.35	72.847	0.00	1.00
WNV ~ Random effects + GMRF		303.87	257.93	72.716	110.64	0.00
WNV ~ Fixed effects + GMRF			339.83	70.583	287.75	0.00
WNV ~ 1 + GMRF			399.10	70.772	414.82	0.00
WNV ~ Fixed effects + Random effects		372.96		7.528	16681.28	0.00
WNV ~ Random effects		361.67		3.558	19012.04	0.00
WNV ~ 1	7602				20213.74	0.00
Monthly						
WNV ~ Fixed effects + Random effects + GMRF		304.65	231.35	22.478	0.00	1.00
WNV ~ Random effects + GMRF		304.07	257.92	22.026	483.85	0.00
WNV ~ Fixed effects + GMRF			339.76	20.087	550.00	0.00
WNV ~ 1 + GMRF			399.02	19.697	1014.90	0.00
WNV ~ Fixed effects + Random effects		372.96		7.823	4314.66	0.00
WNV ~ Random effects		361.67		3.558	6769.80	0.00
WNV ~ 1	60574				7971.50	0.00

SI Table 2. Log likelihoods of spatiotemporal GMRF models at both seasonal and monthly timescales. These likelihoods are gathered from the training model as well as a two-fold cross validation of the training and hold-out data subsets (yielding the “Out-of-sample” and “Within-sample” likelihoods, as well as their “Total sum”).

Source	**Log-likelihoods**	
	Seasonal	Monthly
Out-of-sample	-2407.618	-3991.648
Within-sample	-9264.887	-16952.250
Total sum	-11672.510	-20943.900
Training	-5594.774	-11715.890

Supplemental Information Figures:

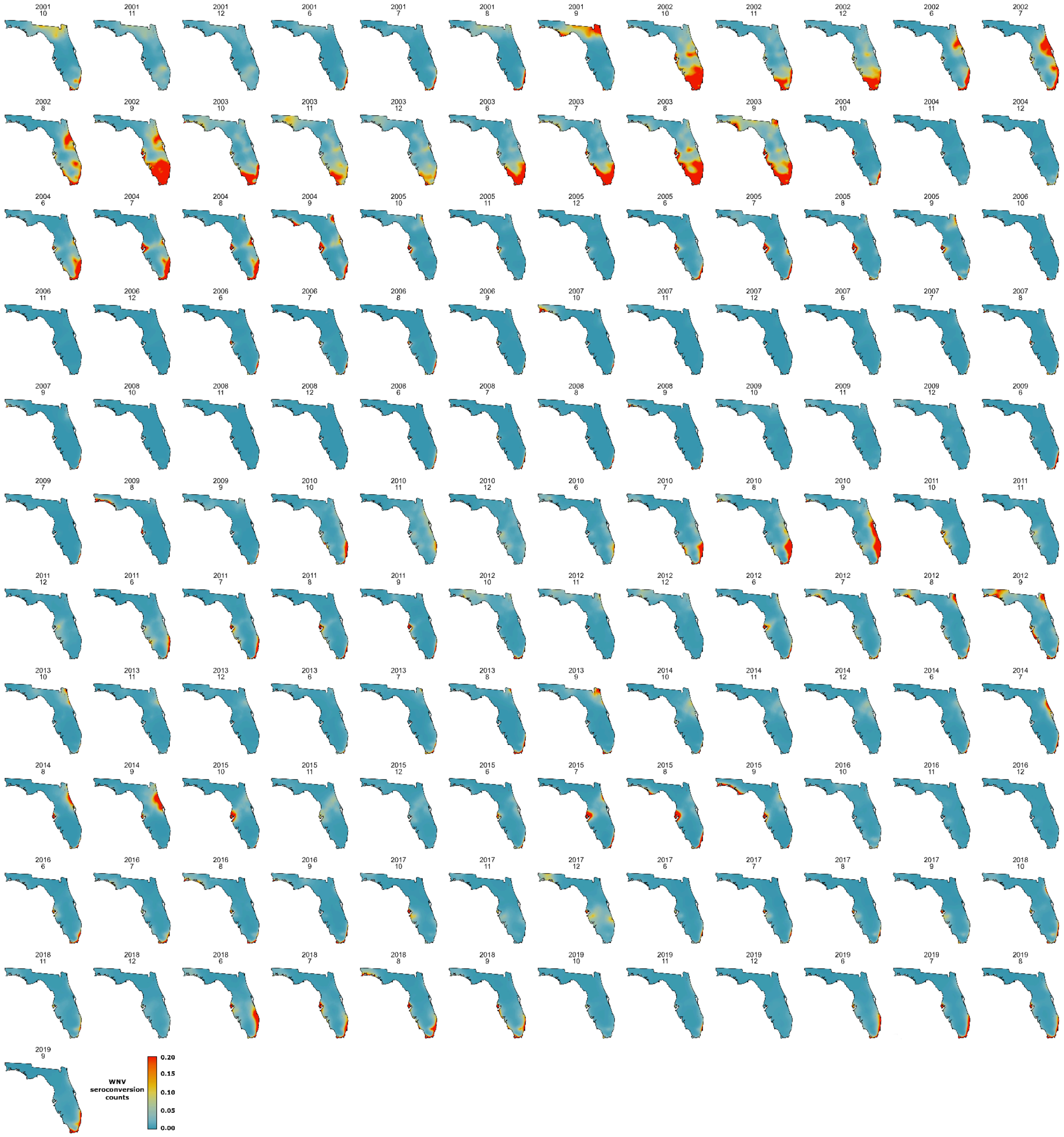

Fig. 1. Statewide predictions of the spatiotemporal dynamics of West Nile Virus seropositive counts from the Florida sentinel chicken system during the years of 2001 – 2019. Predictions were obtained from a spatiotemporal model fitted to data aggregated to monthly counts of WNV seroconversion in a sentinel chicken system during the WNV activity season (June – December). All predictions are provided with a quantile truncation for ease of visualization (98th percentile).